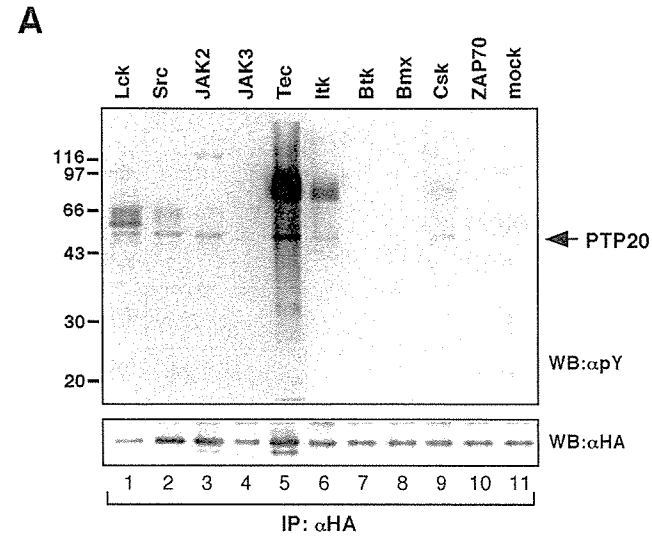

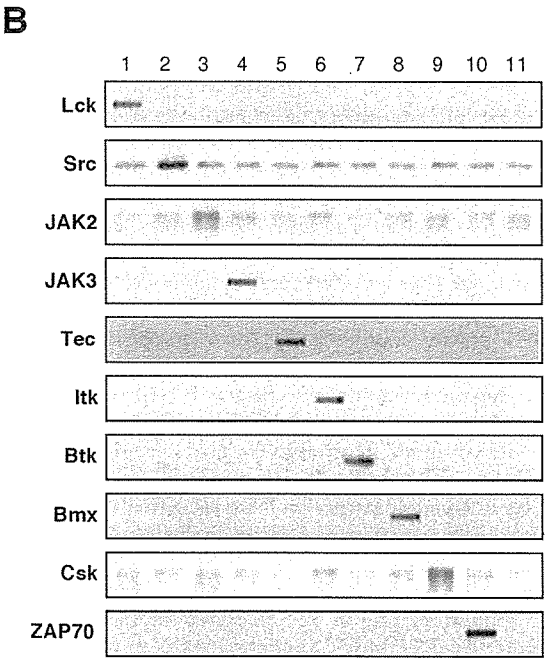

FIG. 1. **Tyrosine phosphorylation of PTP20 by various PTKs.** *A*, COS7 cells were transiently transfected with HA-PTP20 C/S together with either Lck, Src, JAK2, JAK3, Tec, Itk, Btk, Bmx, Csk, or ZAP70. Cells were lysed, and PTP20 was immunoprecipitated (*IP*) with anti-HA antibody followed by immunoblotting (*WB*) with anti-phosphotyrosine antibody (PY99 (*αpY*)). The same membrane was reprobed with anti-HA antibody after stripping. *B*, an aliquot of the cell lysates was immunoblotted with the indicated antibodies to confirm substantial expression of each PTK.

sibly activation. These results suggest that PTP20 is a substrate of Tec and that Tec is also a substrate of PTP20.

Phosphotyrosine-dependent Interaction between PTP20 and Tec—Tec is composed of several distinct domains including pleckstrin homology (*PH*), Tec homology (*TH*), SH3, SH2, and kinase (*KD*) domains (Fig. 3, *panel A*). All of these domains are necessary for full function of Tec under physiological conditions (15, 16). To examine which domains are involved in interaction with PTP20, Tec mutants each lacking one of the domains were co-transfected with the catalytically inactive form of PTP20 into COS7 cells. A kinase mutant as well as two mutants (Y187F and Y518F) where tyrosine residues were replaced by phenylalanines were also included. Cells were lysed, and PTP20 was immunoprecipitated followed by immunoblotting with anti-phosphotyrosine antibody. PTP20 was tyrosine-phosphorylated by the Y187F mutant as well as mutants lacking PH, TH, and SH3 domains to a similar extent as compared with Tec WT (Fig. 3, *panel B*). As expected, the Y518F mutant, which is missing the autophosphorylation site for Tec activation, and the inactive mutant of a kinase mutant could not tyrosine phosphorylate PTP20. Interestingly, the ΔPH mutant could tyrosine phosphorylate PTP20 but was not co-immunoprecipitated with PTP20. Most strikingly, the ΔSH2 mutant could not tyrosine phosphorylate PTP20 and was not co-immunoprecipitated with PTP20. When a membrane on which aliquots of total cell lysates were blotted was probed with anti-phosphotyrosine antibody, it was revealed that co-expression of the Tec ΔSH2 mutant and PTP20 resulted in no tyrosine phosphorylation on both molecules and that the Tec ΔPH mutant tyrosine-phosphorylated (Fig. 3, *panel C*). Tec SH2 domain-dependent interaction with PTP20 was further investigated by co-transfecting the PTP20 C/S mutant with plasmids encoding GST fusion proteins of Tec domains in the presence or absence of Tec into COS7 cells. Cell lysates were subjected to pull-down experiments with GSH-Sepharose beads. Precipitates were separated by SDS-PAGE followed by immunoblotting with the indicated antibodies. In the absence of full-length Tec co-expression, no substantial binding of PTP20 to any of the Tec domains was apparent (Fig. 3, *panel D*). In contrast, in the presence of full-length Tec, phosphorylated PTP20 bound to only the SH2 domain of Tec. Given that co-expression of Tec should result in marked tyrosine phosphorylation of PTP20 in COS7 cells, these data indicate that the PTP20-Tec interaction is mediated predominantly by the SH2 domain of Tec and phosphotyrosine residues of PTP20.

Next, we tried to identify the binding site(s) for Tec in PTP20. Because the interaction of Tec with PTP20 was mediated by the Tec SH2 domain, potential tyrosine residues of phosphorylation were first taken into consideration. There are 13 tyrosine residues (Tyr-62, Tyr-68, Tyr-86, Tyr-101, Tyr-144, Tyr-192, Tyr-244, Tyr-281, Tyr-285, Tyr-303, Tyr-354, Tyr-381, Tyr-419) in the PTP20 sequence, and all the residues are perfectly conserved among human and mouse orthologs (Fig. 4). We focused our attention on the tyrosine residues Tyr-281, Tyr-285, Tyr-303, Tyr-354, Tyr-381, and Tyr-419 located in the C-terminal PEST domain of PTP20, and 6 residues were individually mutated.

First, the mutants were tested for the extent of tyrosine phosphorylation by Tec in transfected COS7 cells. Total cell lysates were subjected to anti-phosphotyrosine blotting. Fig. 5, *panel A*, demonstrates that the PTP20 mutants (Y281F, Y303F, Y354F, Y381F) in which Tyr-281, Tyr-303, Tyr-354, and Tyr-381 were individually mutated exhibited dramatic reduction in tyrosine phosphorylation levels, whereas no apparent reduction for Y285F and Y419F was observed. Combinational mutation of Tyr-281, Tyr-303, Tyr-354, and Tyr-381 totally abolished tyrosine phosphorylation of PTP20. In keeping with these data, anti-phosphotyrosine blotting also demonstrated that tyrosine phosphorylation of Tec was concomitantly reduced. This observation was further extended by GST pull-down experiments using the Tec SH2 domain. COS7 cells were then transfected with PTP20 YF variants together with Tec and Tec-Tec SH2, as outlined in Fig. 3, *panel C*. Mutation of either Tyr-281, Tyr-303, Tyr-354, or Tyr-381 of PTP20 resulted in reduced binding capacity of PTP20 to the Tec SH2 domain, and again, such binding was completely abrogated by substituting all the tyrosine residues (Fig. 5, *panel B*). Together these data clearly indicate that four tyrosine residues in the C-ter-

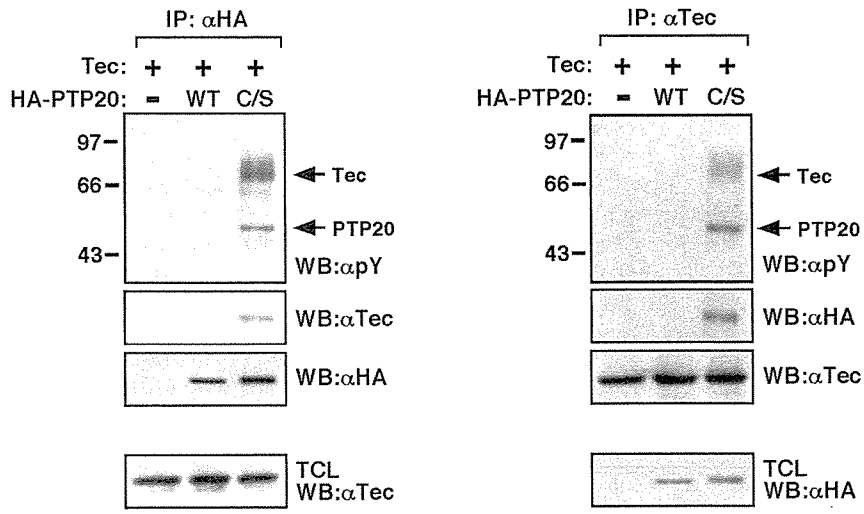

FIG. 2. **Tyrosine phosphorylation-dependent interaction of PTP20 with Tec.** Tec cDNA was transiently introduced into COS7 cells together with either empty vector (mock), HA-PTP20 WT, or C/S and lysed. PTP20 or Tec was immunoprecipitated either with anti-HA (*left panels*) or anti-Tec (*right panels*) antibody, respectively. The immunoprecipitates (*IP*) were separated by SDS-PAGE followed by immunoblotting (*WB*) sequentially with the indicated antibodies. The bands corresponding to Tec and PTP20 are indicated by *arrows*. In either case expression of Tec or HA-PTP20 was confirmed using aliquots of total cell lysates (*TCL*) by immunoblotting (*lowest panels*). *αpY*, anti-phosphotyrosine antibody.

minal non-catalytic region of PTP20 are involved in not only binding to the Tec SH2 domain but also in the phosphorylation and subsequent activation of Tec.

We asked whether the C-terminal non-catalytic region of PTP20 was enough for phosphorylation and activation of Tec. To this end, PTP20 deletion mutants lacking either an N-terminal catalytic or a C-terminal non-catalytic segment were made, but the resultant constructs could not be expressed in COS7 cells, although comparable amounts of transcripts were detected (data not shown). To solve this problem, the N-terminal PTP domain and the C-terminal PEST domain were inserted into pEBG vector and were expressed as GST fusion proteins in COS7 cells. These pEBG plasmids encoding the PTP domain and full length of PTP20 C/S mutant and the PEST domain of PTP20 were co-transfected into COS7 together with Tec. Anti-phosphotyrosine blotting documented that Tec was highly tyrosine-phosphorylated with the full-length but not the PTP domain of the PTP20 C/S mutant (Fig. 6, *panel A*), supporting previous data shown in Fig. 5, where the C-terminal part of PTP20 was essential for tyrosine phosphorylation of Tec. Interestingly, the presence of the PEST domain of PTP20 caused tyrosine phosphorylation of PTP20, but the extent was lower than in the presence of the full-length PTP20 C/S mutant. Equivalent expression of each construct was confirmed by Western blotting with anti-Tec and anti-GST antibodies. To further examine the involvement of the PEST domain, lysates were precipitated with GSH-Sepharose beads followed by immunoblotting with anti-phosphotyrosine antibody. A phosphorylated 74-kDa band, which was shown to be Tec by immunoblotting, was co-precipitated with full-length PTP20 C/S mutant, whereas the PTP domain alone could not capture Tec (Fig. 6, *panel B*). A faint tyrosine-phosphorylated band with the same mobility of 74 kDa that co-precipitated with the PEST domain appeared to be Tec but could not be detected by our anti-Tec antibody presumably due to sensitivity. These results suggest that the PEST domain of PTP20 is necessary but not sufficient for not only hyperphosphorylation and activation of, but also association with Tec.

Negative Regulatory Roles of PTP20 in BCR Signaling—All the experiments documented above were conducted in transfected COS7 cells. To demonstrate a physiological relevance of the PTP20-Tec interaction, evidence of such an association in non-transfected cells was required. To this end we selected human Ramos immature B cells, because it has been reported that they express relatively high amounts of endogenous Tec (21). As shown above, interaction of PTP20 with Tec is mediated by tyrosine phosphorylation of PTP20, and PTP20 has autodephosphorylation activity, implying that it would be difficult to detect a phosphotyrosine-dependent interaction of PTP20 with other molecules including Tec endogenously. To overcome this experimental difficulty, protein-tyrosine phosphorylation was induced in Ramos cells by treatment with pervanadate (POV). Cells were starved for 16 h in serum-free medium and then either left unstimulated or treated with 0.1 mM POV for 30 min and lysed. Cell lysates were immunoprecipitated with either anti-phosphotyrosine antibody or anti-Tec antibody. Our PTP20-specific antibody could not be used due to its inability in immunoprecipitation experiments. In anti-phosphotyrosine immunoprecipitates, specific bands with 74 and 50 kDa corresponding to human Tec and PTP20 were detected only upon POV treatment (Fig. 7). A tyrosine-phosphorylated band with 50 kDa in the anti-Tec immunoprecipitates was readily detected by the anti-PTP20 antibody but only when cells received POV pretreatment (Fig. 7). These results indicate that endogenous Tec and PTP20 interact with each other in a phosphotyrosine-dependent manner in Ramos B cells.

Although upstream regulators such as cytokine receptors, lymphocyte surface antigens, G protein-coupled receptors, receptor type PTKs, or integrins for Tec in blood cells including Ramos B cells have been relatively well investigated (13, 20, 22–26), only limited information regarding downstream regulators of Tec has been available so far. If the data obtained in transfected COS7 cells are true, PTP20 would be thought to play a negative regulatory role in Tec-mediated signaling. To examine this, either the PTP20 WT, the inactive C/S mutant, or another form of catalytically inactive mutant D/A was transiently co-transfected with the pfos/luc reporter plasmid into Ramos cells, because the promoter of the c-*fos* proto-oncogene is activated in response to BCR cross-linking in the cells. Cells were either left unstimulated or treated with anti-human IgM $F(ab')_2$ fragments for 5 h. Cell lysates were assayed for luciferase activity. BCR cross-linking induced a marked activation of the c-*fos* promoter (Fig. 8). Expression of PTP20 WT totally inhibited BCR-induced activation of the c-*fos* promoter as well as its basal activity, whereas only about 20% inhibition of the promoter activation was observed in the co-expression of catalytically inactive forms of PTP20, strongly indicating that PTP20 is a negative regulator of BCR-Tec-c-*fos* signaling.

Tyrosine Phosphorylation of PTP20 by Tec Modulates Its Catalytic Activity against Tec as Well as Itself—We demonstrated that specific tyrosine residues Tyr-281, Tyr-303, Tyr-354, and Tyr-381 of PTP20 could be phosphorylated by Tec and served as Tec binding sites (Fig. 5). To further investigate physiological relevance of PTP20 tyrosine phosphorylation, substitution of the tyrosine residues with phenylalanine in PTP20 WT was performed. The YF mutants of HA-PTP20 WT

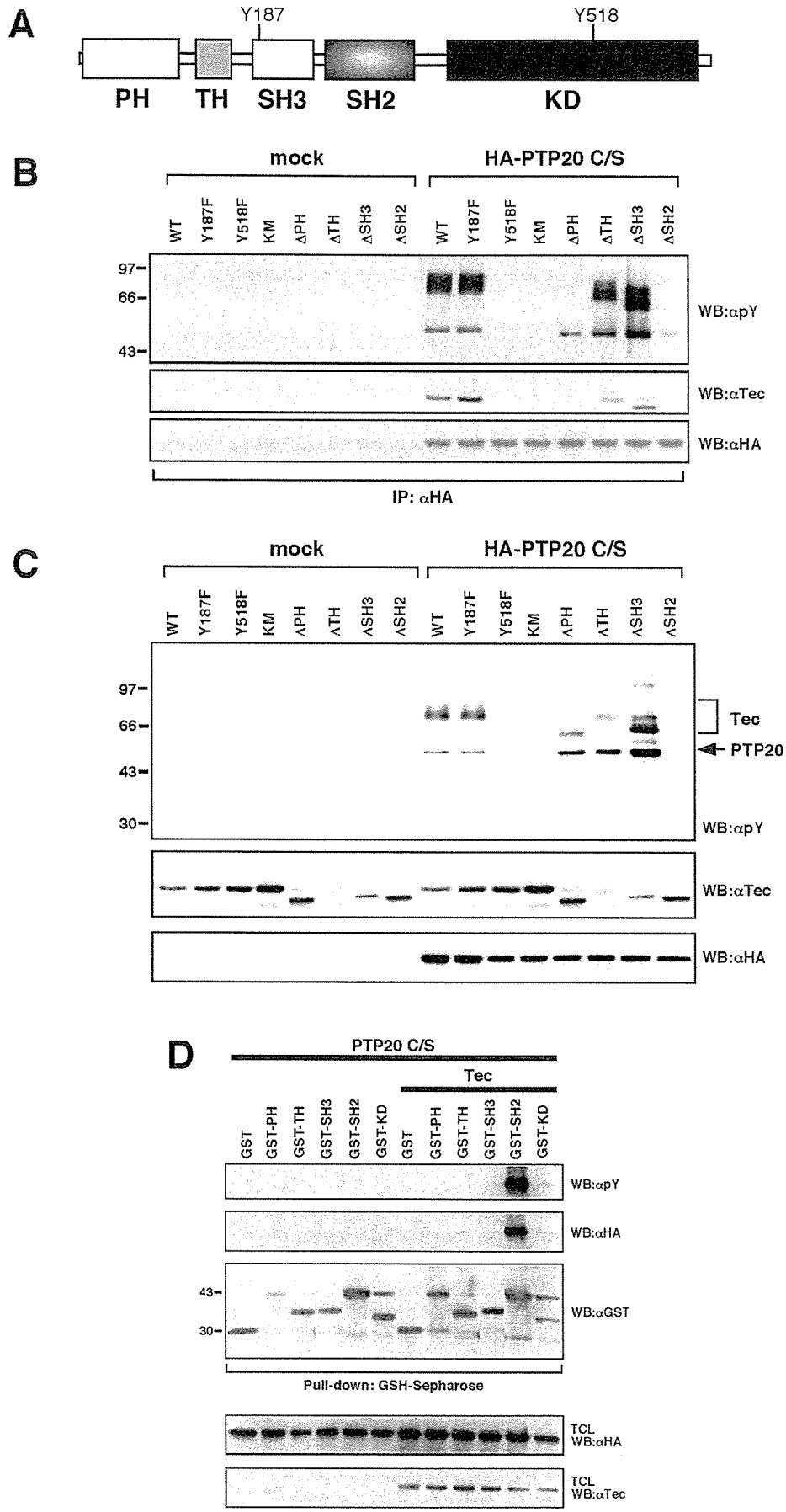

FIG. 3. **Tec SH2 domain is essential for both tyrosine phosphorylation of PTP20 and association of Tec with PTP20.** *A*, schematic organization of mouse Tec into PH, TH, SH3, SH2, and kinase (*KD*) domains. *B*, COS7 cells were transiently transfected with either empty vector (*mock*) or HA-PTP20 C/S together with the indicated Tec mutants. Cells were lysed, and HA-PTP20 was immunoprecipitated (*IP*) followed by immunoblotting (*IB*) with anti-phosphotyrosine antibody (PY99 (*αpY*)). The same membrane was sequentially reprobed with anti-Tec and anti-HA antibodies after stripping. *C*, aliquots of the total cell lysates (*TCL*) were separated by SDS-PAGE followed by immunoblotting with indicated antibodies. *D*, COS7 cells were transiently transfected with pEBG empty vector (GST) or bearing each of Tec domains (PH, TH, SH3, SH2, and KD) in the absence or presence of Tec plasmid. Cells were lysed, and GST fusion proteins were precipitated by GSH-Sepharose beads followed by immunoblot analysis with anti-phosphotyrosine (*pY*) antibody. The same membrane was sequentially reprobed with indicated antibodies. Expression of PTP20 and Tec was confirmed using aliquots of total cell lysates (*TCL*) by immunoblotting as indicated.

```
PTP20(rat)   MSRQSDLVRS FLEQQEARDH RKGAILAREF SDIKARSVAW KTEGVCSTKA GSQQGNSKKN  60
HSCF(mouse)  MSRHTDLVRS FLEQLEARDY REGAILAREF SDIKARSVAW KSEGVCSTKA GSRLGNTNKN  60
BDP1(human)  MSRSLDSARS FLERLEARGG REGAVLAGEF SDIQACSAAW KADGVCSTVA GSRPENVRKN  60

                62     68                      86                 101
PTP20(rat)   RYKDVVPYDE TRVILSLLQE EGHGDYINAN FIRGTDGSQA YIATQGPLPH TLLDFWRLVW 120
HSCF(mouse)  RYKDVVAYDE TRVILSLLQE EGHGDYINAN FIRGIDGSQA YIATQGPLPH TLLDFWRLVW 120
BDP1(human)  RYKDVLPYDQ TRVILSLLQE EGHSDYINGN FIRGVDGSLA YIATQGPLPH TLLDFWRLVW 120

                                        144
PTP20(rat)   EFGIKVILMA CQETENGRRK CERYWAQERE PLQAGPFCIT LTKETALTSD ITLRTLQVTF 180
HSCF(mouse)  EFGVKVILMA CQETENGRRK CERYWAREQE PLKAGPFCIT LTKETTLNAD ITLRTLQVTF 180
BDP1(human)  EFGVKVILMA CREIENGRKR CERYWAQEQE PLQTGLFCIT LIKEKWLNED IMLRTLKVTF 180

                       192
PTP20(rat)   QKESRPVHQL QYMSWPDHGV PSSSDHILTM VEEARCLQGL GPGPLCVHCS AGCGRTGVLC 240
HSCF(mouse)  QKEFRSVHQL QYMSWPDHGV PSSSDHILTM VEEARCLQGL GPGPLCVHCS AGCGRTGVLC 240
BDP1(human)  QKESRSVYQL QYMSWPDRGV PSSPDHMLAM VEEARRLQGS GPEPLCVHCS AGCGRTGVLC 240

               244                                      281 285
PTP20(rat)   AVDYVRQLLL TQTIPPNFSL FEVVLEMRKQ RPAAVQTEEQ YRFLYHTVAQ LFSRTLQNNS 300
HSCF(mouse)  AVDYVRQLLL TQTIPPNFSL FQVVLEMRKQ RPAAVQTEEQ YRFLYHTVAQ LFSRTLQDTS 300
BDP1(human)  TVDYVRQLLL TQMIPPDFSL FDVVLKMRKQ RPAAVQTEEQ YRFLYHTVAQ MFCSTLQNAS 300

                303                                                  354
PTP20(rat)   PLYQNLKENR APICKDSSSL RTSSALPATS RPLGGVLRSI SVPGPPTLPM ADTYAVVQKR 360
HSCF(mouse)  PHYQNLKENC APICKEAFSL RTSSALPATS RPPGGVLRSI SVPAPPTLPM ADTYAVVQKR 360
BDP1(human)  PHYQNIKENC APLYDDALFL RTPQALLAIP RPPGGVLRSI SVPGSPGHAM ADTYAVVQKR 360

                                        381
PTP20(rat)   GASGSTGPGT RAPNST---- --DTPIYSQV APRIQRPVSH TENAQGTTAL GRVPADENPS 414
HSCF(mouse)  GASAGTGPGP RAPTST---- --DTPIYSQV APRAQRPVAH TEDAQGTTAL RRVPADQNSS 414
BDP1(human)  GAPAGAGSGT QTGTGTGARS AEEAPLYSKV TPRAQRPGAH AEDARGTLP- GRVPADQSPA 420

               419
PTP20(rat)   GPDAYEEVTD GAQTGGLGFN LRIGRPKGPR DPPAEWTRV 453
HSCF(mouse)  GPDAYEEVTD GAQTGGLGFN LRIGRPKGPR DPPAEWTRV 453
BDP1(human)  GSGAYEDVAG GAQTGGLGFN LRIGRPKGPR DPPAEWTRV 458
```

FIG. 4. **Sequence alignment of PTP20 with its human (brain-derived phosphatase 1 (*BDP1*)) and mouse (*HSCF*) orthologs.** The 13 conserved tyrosine residues are *boxed* and *numbered* based on the amino acid sequence of PTP20. PTP catalytic domains are indicated by *gray shading*.

were co-transfected with Tec and the PTP20 C/S mutant without epitope tagging, and effects on the extent of tyrosine phosphorylation on Tec were analyzed by anti-phosphotyrosine blotting. As shown in Fig. 9*A*, substitution of Tyr-281 with phenylalanine (Y281F) resulted in dramatic loss of PTP20 dephosphorylation activity against Tec. On the other hand, Tec could be dephosphorylated by Y303F, Y354F, and Y381F to nearly the same extent by PTP20 WT. The PTP20 Y281F/Y303F/Y354/F381F mutant in which 4 tyrosine residues were substituted by phenylalanine also exhibited apparently no dephosphorylation activity against Tec. Equivalent expression of HA-PTP20 was confirmed by immunoblotting (*lowest panel*). Next, the autodephosphorylation activity of the YF mutants of HA-PTP20 WT was assessed by co-transfecting Tec and-PEST encoding the GST-PTP20 PEST domain into COS7 cells, as GST-PTP20 PEST alone became tyrosine-phosphorylated in the presence of Tec (Fig. 6). Cells were lysed and GST-PTP20 PEST was precipitated with GSH-Sepharose beads followed by anti-phosphotyrosine blotting. Again, PTP20 Y281F as well as PTP20 Y281F/Y303F/Y354/F381F showed no dephosphorylation activity against GST-PTP20 PEST, whereas PTP20 Y303F, Y354F, and Y381F as well as PTP20 WT could dephosphorylate GST-PTP20 PEST (Fig. 9*B*). These YF mutants also were transfected into Ramos B cells, and c-*fos* promoter activity was assayed after BCR ligation. Ectopic expression of PTP20 Y281F and Y281F/Y303F/Y354/F381F mutants still inhibited c-*fos* promoter activity (about 50%, relative to mock transfectants), but the extent was significantly lower than that of WT as well as other YF mutants. These results strongly suggest that phosphorylation of Tyr-281 on PTP20 is essential for expression of catalytic activity against not only Tec but also PTP20 itself in transfected COS7 cells as well as in Ramos B cells, although other tyrosine residues, Tyr-303, Tyr-354, and Tyr-381, are also phosphorylated by Tec.

DISCUSSION

Many signaling pathways triggered by PTKs can be potentially modulated by PTPs in a negative or positive manner under cellular context. In some cases phosphorylation on the tyrosine residues of PTPs themselves can modulate their catalytic activities. For example, SH2 domain-containing PTP SHP-2 is tyrosine-phosphorylated upon stimulation by a variety of growth factors (27–29) and cytokines (30–35). Once SHP-2 becomes tyrosine-phosphorylated, their catalytic activity might be increased and modulated its own tyrosine phosphorylation level by autodephosphorylation activity (36, 37). It also has been reported that tyrosine phosphorylation of PTP1B upon insulin and epidermal growth factor treatment causes reduction in its catalytic activity, thereby enhancing apparent insulin receptor- and epidermal growth factor receptor-mediated signaling pathways (38, 39). Thus, tyrosine phosphorylation of PTPs appeared to be critical for the regulation of their biological functions.

Among the PEST family PTPs, PTP20 is an only member that gets phosphorylated on tyrosine residues, whereas no tyrosine phosphorylation of other members, PTP-PEST and PTP-

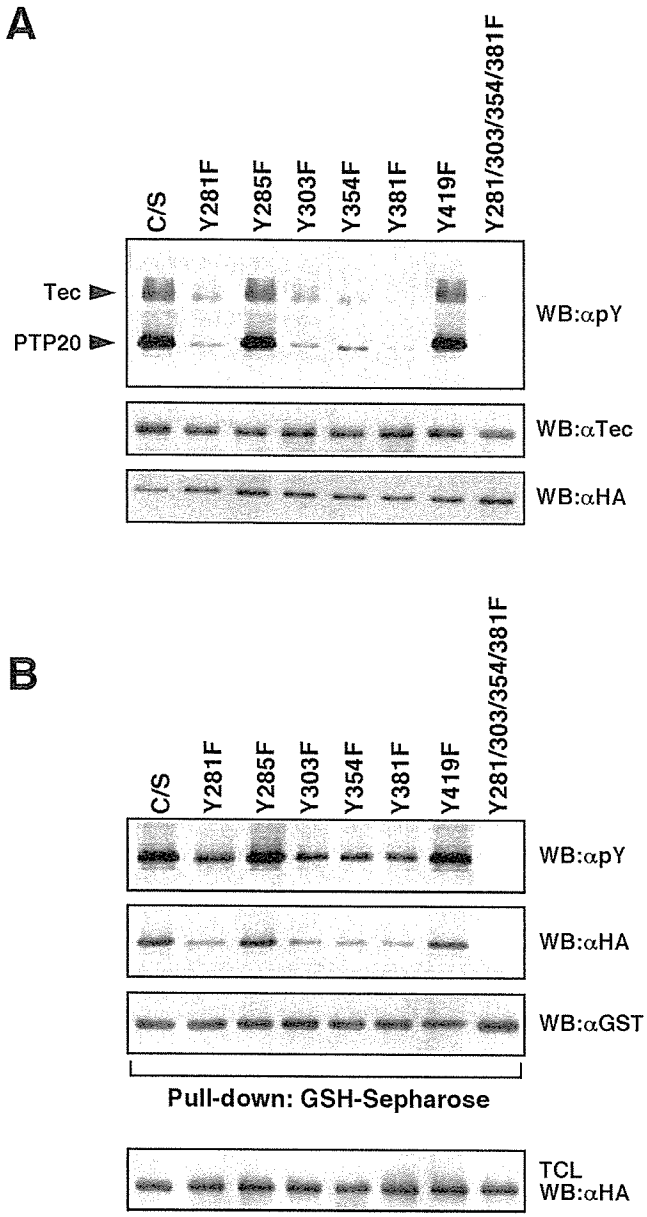

FIG. 5. **Specific tyrosine residues of PTP20 are necessary for tyrosine phosphorylation of Tec and association with Tec SH2 domain.** *A*, HA-PTP20 C/S or its YF (tyrosine to phenylalanine substitution) mutants as indicated were co-transfected into COS7 cells with Tec. Aliquots of total cell lysates (*TCL*) were immunoblotted (*WB*) with anti-phosphotyrosine (*αpY*) antibody. The same membrane was sequentially reprobed with anti-Tec and -HA antibodies. *B*, COS7 cells were co-transfected with expression plasmids for HA-PTP20 C/S or its YF mutants, Tec, and GST-Tec-SH2 domain. Cells were lysed, and GST-Tec-SH2 domain was precipitated with GSH-Sepharose beads followed by immunoblot analysis by sequential probing with anti-phosphotyrosine, anti-HA, and anti-GST antibodies. Expression of nearly the same amounts of PTP20 was confirmed by immunoblotting of aliquots of total cell lysates with anti-HA antibody.

PEP, has been reported. In the present study, we clearly demonstrated that PTP20 was tyrosine-phosphorylated by a cytosolic Tec kinase. As previously reported for phosphorylation of PTP20 by constitutively active Src family kinases (8, 11), the catalytically inactive form of PTP20 was found to be tyrosine-phosphorylated to a greater extent by Tec, whereas apparently no phosphorylation on PTP20 WT was obvious, possibly due to its autodephosphorylation activity. Src and Lck indeed tyrosine-phosphorylated PTP20, but the extent of tyrosine phosphorylation of PTP20 by Tec was shown to be the greatest (Fig. 1). Moreover, related Itk did tyrosine-phosphorylate PTP20 to a lesser extent, but Btk and Bmx did not (Fig. 1). These results suggest that Tec kinase tyrosine phosphorylates PTP20 more specifically and preferentially than Src family kinases and its related kinases do.

Without ectopic PTP20 expression, tyrosine phosphorylation of Tec kinase was not detected in transfected COS7 cells (Fig. 2). Although co-expression of PTP20 WT did not induce tyrosine phosphorylation of Tec, the catalytically inactive C/S variant of PTP20 caused tyrosine phosphorylation of Tec and co-immunoprecipitated with Tec. These results strongly suggest that a dominant-negative effect of PTP20 C/S expression on Tec tyrosine phosphorylation seems to be unlikely and, rather, that Tec was possibly autophosphorylated and further activated by interacting with PTP20 and then was immediately dephosphorylated and deactivated by PTP20, which might also be activated through interaction with Tec in a tyrosine phosphorylation-dependent manner. A deletion of the Tec SH2 domain abrogated tyrosine phosphorylation of Tec as well as PTP20 and association between Tec and PTP20 (Fig. 3). Likewise, substitution of individual tyrosine residues Tyr-281, Tyr-303, Tyr-354, and Tyr-381 with phenylalanines of PTP20 reduced not only tyrosine phosphorylation of Tec and PTP20 itself but also association of PTP20 with the Tec SH2 domain (Fig. 5). Substitution of all the four tyrosine residues (Fig. 5) as well as a deletion of the C-terminal non-catalytic segment (Fig. 6) completely abolished those events, and the C-terminal segment alone partially induced Tec tyrosine phosphorylation (Fig. 6), supporting the idea that phosphotyrosine-dependent interaction between PTP20 and Tec is essential for determining a mutual state of phosphorylation and activation. Taken together, we propose a working hypothesis of tyrosine phosphorylation-dependent interaction between PTP20 and Tec kinase (Fig. 10).

PTPs exhibit elaborate substrate specificity *in vivo*. This specificity can be achieved at two levels. First, the phosphatase catalytic domain itself displays an intrinsic specificity for its substrate. However, the affinity between the catalytic domain and its substrate is often low. Actually, the PTP domain of the catalytically inactive PTP20 alone could not capture a potential substrate Tec kinase (Fig. 6). A further enhancement of the specificity is achieved by protein-protein targeting; the Tec SH2 domain and phosphorylated tyrosine residues on PTP20 could enhance the interaction between the two molecules. In Ramos B cells, we could detect tyrosine phosphorylation-dependent interaction between PTP20 and Tec only when cells were treated with pervanadate (Fig. 7). In this case, however, apparent binding might have resulted from a sole interaction of phosphorylated tyrosines of PTP20 C-terminal with the Tec SH2 domain and, therefore, underestimated because vanadate can get into the catalytic pocket of PTP20 reversibly and inhibit interaction between the PTP domain segment of PTP20 and tyrosine-phosphorylated Tec kinase. Upon physiological stimulation both PTP20 catalytic domain-Tec phosphotyrosine(s) and PTP20 phosphotyrosine-Tec SH2 domain bindings could play an essential role.

Most interestingly, tyrosine phosphorylation of PTP20 appears to regulate its catalytic activity against Tec and PTP20 itself. Among the tyrosine residues phosphorylated by Tec kinase, tyrosine 281 might be critical for dephosphorylation activity of PTP20 in transfected COS7 cells as well as in Ramos B cells (Fig. 9). In the case of ectopic expression in COS7 cells, substitution of the Tyr-281 nearly abolished dephosphorylation activity against both PTP20 and Tec (Fig. 9, *A* and *B*). On the other hand Y281F as well as Y281F/Y303F/Y354/F381F mutants exhibited reduced, but still ~50% dephosphorylation activity as compared with mock transfectants when expressed in

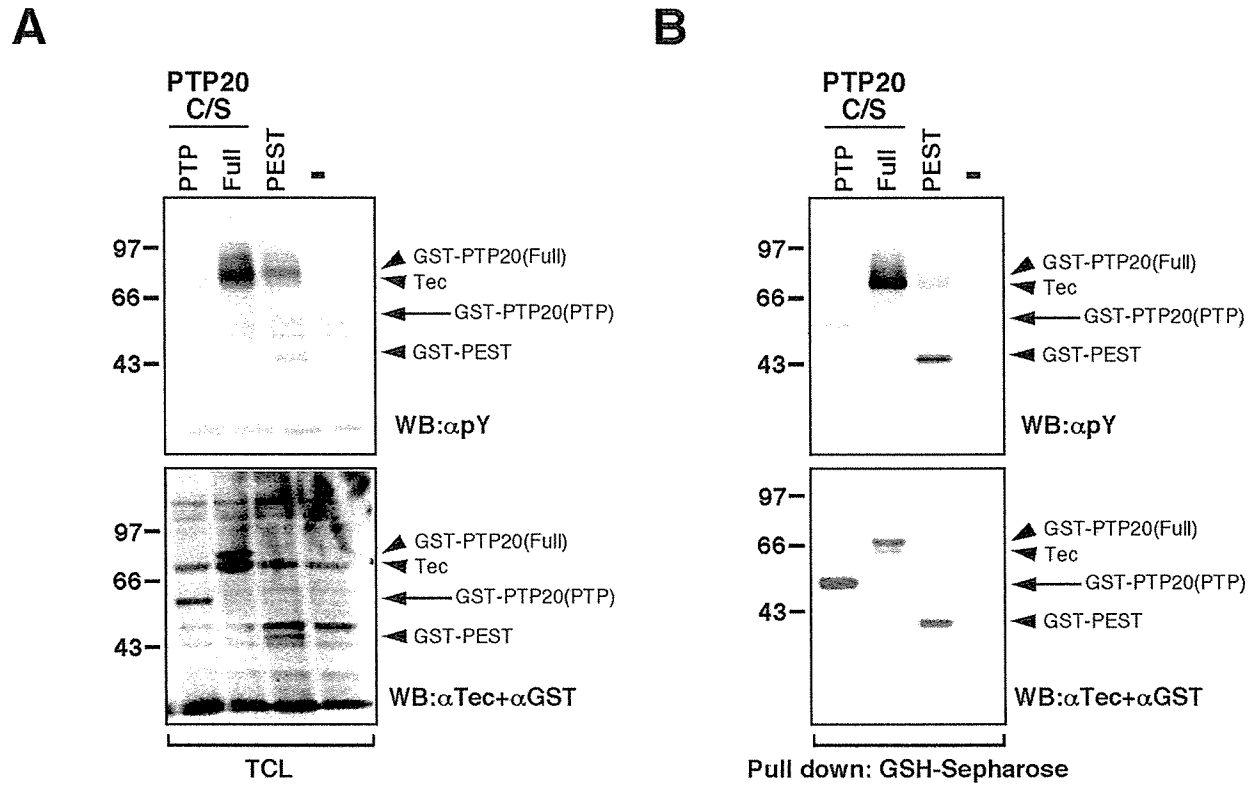

FIG. 6. **Both PTP catalytic and PEST domains of PTP20 are involved in maximal phosphorylation of Tec and association with Tec.** Tec was co-transfected with either empty pEBG vector (−) or that bearing the PTP20 catalytic domain (*PTP*), full-length PTP20 (*Full*), or the non-catalytic PEST domain of PTP20 (*PEST*). *A*, aliquots of total cell lysates (*TCL*) were subjected to immunoblotting with anti-phosphotyrosine antibody (*αpY*, *upper panel*). The same membrane was reprobed with a mixture of anti-Tec and anti-GST antibodies. *B*, remaining cell lysates were precipitated with GSH-Sepharose beads and processed as mentioned above. The bands corresponding to individual products are indicated by *arrows*.

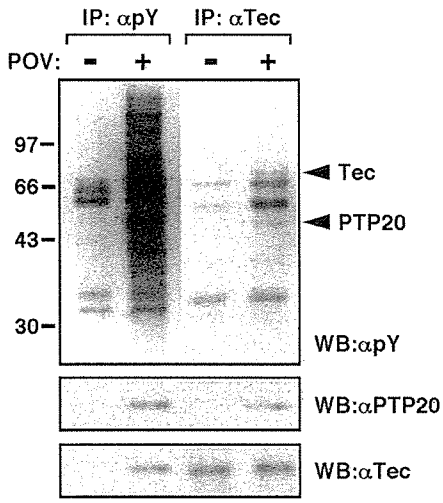

FIG. 7. **Tyrosine phosphorylation-dependent interaction of endogenous PTP20 with endogenous Tec in Ramos B cells.** Ramos cells were treated with 0.1 mM POV for 15 min at 37 °C, lysed, and subjected to immunoprecipitation with either anti-phosphotyrosine (*αpY*) or anti-Tec antibody. The immunoprecipitates (*IP*) were immunoblotted (*WB*) by anti-phosphotyrosine antibody. The same membranes were sequentially reprobed with anti-PTP20 and -Tec antibodies. The bands corresponding to Tec and PTP20 are indicated by *arrowheads*.

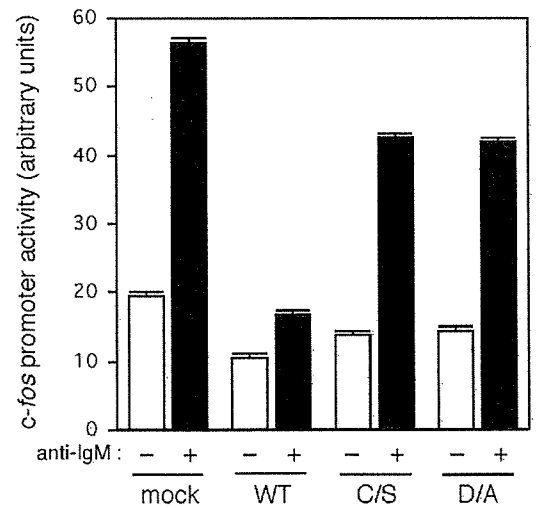

FIG. 8. **Negative role of PTP20 in BCR signaling.** Ramos cells (1×10^7) were subjected to electroporation with 2 μg of the pfos/luc reporter plasmid together with 10 μg of pcDNA3 vector (mock) or bearing PTP20 WT, C/S, or D/A mutant. Five hours after transfection cells were incubated for an additional 5 h in the absence (*open bars*) or presence (*closed bars*) of anti-IgM (ab') (10 μg/ml). Cells lysates were then assayed for luciferase activity. Data are expressed as mean ± S.D. of triplicate determinations.

Ramos B cells (Fig. 9*C*), suggesting that other direct or indirect mechanisms to regulate PTP20 activity are involved in dephosphorylation and deactivation of Tec in the cells. However, we cannot exclude the possibility that phosphorylation on serine and threonine residues rich in the C-terminal region of PTP20 might affect catalytic activity of PTP20, as PTP20 can be regulated under the control of follicle-stimulating hormone in rat ovarian granulosa cells, where no tyrosine phosphorylation on PTP20 was observed (14).

It has been reported that constitutively active Lck phosphorylates tyrosine residues 354 and 381 on PTP20, which are in turn recognized by the Csk SH2 domain (11). In that report it was also documented that mutation of both the tyrosine resi-

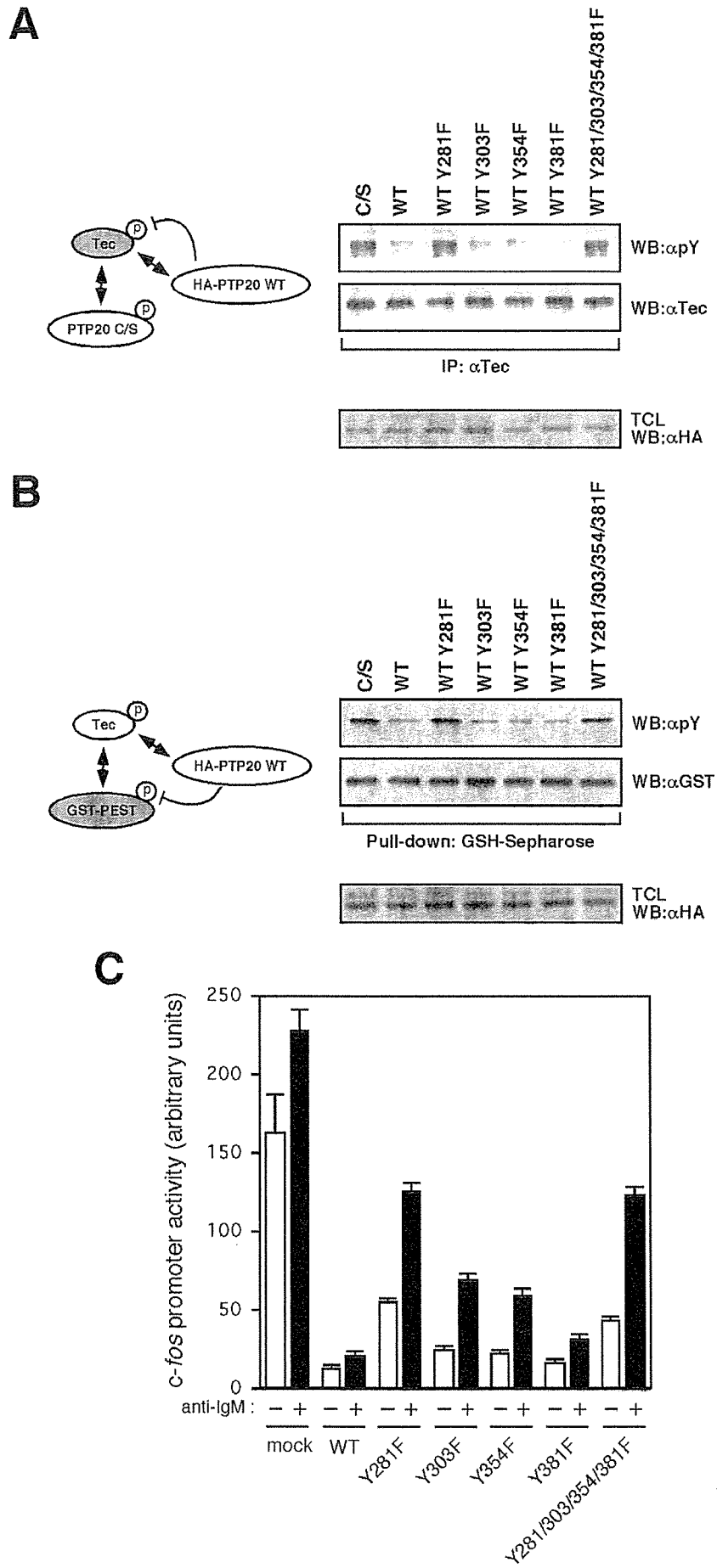

FIG. 9. **Tyrosine 281 is critical for *in vivo* phosphatase activity of PTP20.** *A*, COS7 cells were co-transfected with Tec, PTP20 C/S, and HA-PTP20 WT or its YF mutants. HA-PTP20 C/S was also included as a negative control. Cells were lysed, and Tec was immunoprecipitated with anti-Tec antibody. The immunoprecipitates (*IP*) were separated by SDS-PAGE followed by immunoblotting (*WB*) with indicated antibodies. Expression of HA-PTP20 was confirmed using aliquots of total cell lysates (*TCL*) with anti-HA antibody. *αpY*, anti-phosphotyrosine antibody. *B*, COS7 cells were transfected as above, but PEST-encoding GST-PTP20 PEST domain (GST-PEST) in place of PTP20 C/S was included. Cell lysates were subjected to precipitation with GSH-Sepharose beads and immunoblotted with the indicated antibodies. Expression of HA-PTP20 was confirmed using aliquots of total cell lysates (*TCL*) with anti-HA antibody. *C*, Ramos cells were transfected by electroporation with 2 μg of the pfos/luc reporter plasmid together with 10 μg of pcDNA3 vector (mock) or bearing PTP20 WT or its YF mutant and processed as described in legend to Fig. 8.

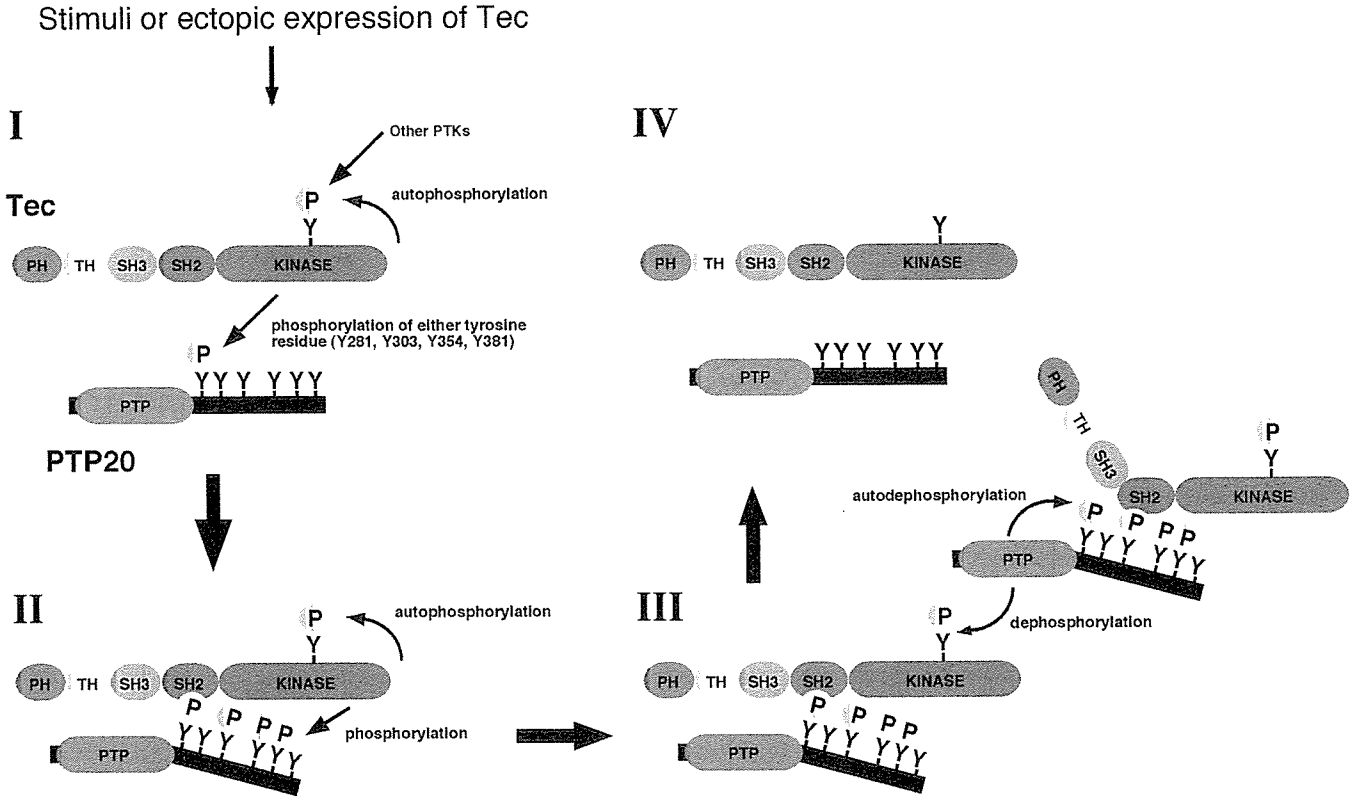

FIG. 10. **Working hypothesis for interaction of PTP20 with Tec.** *I*, upon stimuli or ectopic expression of Tec, Tec becomes tyrosine-phosphorylated and activated through autophosphorylation and other PTK catalytic activity. In turn, Tec phosphorylates tyrosine residues (Tyr-281, Tyr-303, Tyr-354, Tyr-381) on PTP20. *II*, phosphorylated PTP20 associates with Tec SH2 domain of remaining inactive Tec, thereby activating the Tec kinases. Interaction of Tec with PTP20 increases a pool of activated Tec and PTP20. *III*, activated PTP20 by phosphorylation then dephosphorylates Tec as well as PTP20 itself. Note that free of phosphorylated tyrosine 281 from association with Tec SH2 domain might be necessary for expression of PTP20 dephosphorylation activity. *IV*, finally, both Tec and PTP20 return to basal and inactive states.

dues on PTP20 caused no changes in catalytic activity by *in vitro* phosphatase assay. We have also showed that PTP20 was tyrosine-phosphorylated by Lck and Src and was associated with the PTKs (Fig. 2). However, neither the SH2 nor the SH3 domain of Lck was shown to be involved in the association with PTP20 (data not shown). Recently, another cytosolic protein-tyrosine kinase c-Abl also was shown to phosphorylate PTP20 and in turn to be dephosphorylated by PTP20 (10). Although PTP20-Tec and PTP20-cAbl interactions seem to be analogous, association between PTP20 and c-Abl is indirect, and PSTPIP, which is also a substrate of PTP20, instead serves as an adapter by bridging PTP20 to c-Abl. In contrast, association between PTP20 and Tec kinase seems to be direct, and involvement of adaptor molecules such as PSTPIPs is unlikely because the Tec SH2 domain alone could capture tyrosine-phosphorylated PTP20 (Fig. 3*D*) and, consistently, substitution of tyrosine residues on PTP20 dramatically reduced the mutual binding (Fig. 5*B*). These imply that PTP20 might be differentially tyrosine-phosphorylated by Lck, Tec, and c-Abl kinases depending on cellular context.

The Tec kinase was initially isolated from mouse liver (40) and was subsequently shown to be expressed in many tissues, including spleen, lung, brain, and kidney (41). Four Tec-related PTKs, including Btk (42, 43), Itk (also known as Emt or Tsk) (44–46), Bmx (47), and Txk (or Rlk) (48, 49), have also been molecularly cloned. Tec and the related kinases can be activated by cytokine receptors, lymphocyte surface antigens, G protein-coupled receptors, receptor type PTKs, or integrins (13, 20, 22–26). However, little is known about how the inactivation of Tec kinase is achieved. In this study, we have showed that PTP20 is a potential negative regulator in Tec-mediated signaling pathway and that the Tec SH2 domain is essential for the negative regulation by PTP20. Itk, another member of Tec family, might also be regulated by PTP20 in T cells in a similar fashion,[2] whereas Btk and Bmx seem not to interact with PTP20 (Fig. 1). Recently, the Tec SH2 domain has been shown to bind to Dok-1, which is tyrosine-phosphorylated by Tec, causing inhibition of BCR-mediated c-*fos* promoter activation (18). Another publication has demonstrated that a docking protein, BRDG1, binds to the Tec SH2 domain and acts downstream of Tec in a positive fashion in BCR signaling (50). Thus, the Tec SH2 domain might differentially participate in BCR signaling in a positive or negative way.

PTP D1, which comprises another subfamily of cytosolic PTPs, is shown to be a potential regulator and effector for not only Bmx/Etk kinase but also Tec kinase (51). The PH but not SH2 domain of Bmx/Etk is involved in the interaction with the central portion (residues 726–848) of PTP D1, and such binding is phosphotyrosine-independent, unlike PTP20-Tec interaction. Interaction between Bmx/Etk and PTP D1 stimulates the kinase activity of Bmx/Etk, resulting in an increased phosphotyrosine content in both proteins. Although it is obvious that PTP D1 is a substrate of Bmx/Etk and Tec, PTP D1 appears not to dephosphorylate the kinases. Rather, PTP D1 is a positive regulator in Bmx/Etk- and Tec-mediated signaling pathway leading to STAT3 activation. By co-transfection experiments, we observed that PTP36, which belongs to the same PTP subfamily as PTPD1, was tyrosine-phosphorylated by Tec kinase (data not shown). Thus, Tec-mediated signaling could be negatively or positively regulated by interacting with PTPs.

In conclusion, PTP20 appears to play a negative role in the

[2] S. Yamasaki and N. Aoki, unpublished data.

Tec-mediated, in particular in BCR, signaling pathways and the tyrosine phosphorylation-dependent interaction between Tec and PTP20 might form a negative feedback loop. To our knowledge this is the first report demonstrating that tyrosine phosphorylation-dependent interaction between PTK and PTP is relevant for their mutual state in some cellular context.

REFERENCES

1. Andersen, J. N., Mortensen, O. H., Peters, G. H., Drake, P. G., Iversen, L. F., Olsen, O. H., Jansen, P. G., Andersen, H. S., Tonks, N. K., and Moller, N. P. (2001) *Mol. Cell. Biol.* **21,** 7117–7136
2. Tonks, N. K., and Neel, B. G. (2001) *Curr. Opin. Cell Biol.* **13,** 182–195
3. Aoki, N., Yamaguchi-Aoki, Y., and Ullrich, A. (1996) *J. Biol. Chem.* **271,** 29422–29426
4. Cheng, J., Daimaru, L., Fennie, C., and Lasky, L. A. (1996) *Blood* **88,** 1156–1167
5. Huang, K., Sommers, C. L. Grinberg, A. Kozak, C. A. and Love, P. E. (1996) *Oncogene* **13,** 1567–1573
6. Dosil, M., Leibman, N., and Lemischka, I. R. (1996) *Blood* **88,** 4510–4525
7. Kim, Y. W., Wang, H., Sures, I., Lammers, R., Martell, K. J., and Ullrich, A. (1996) *Oncogene* **13,** 2275–2279
8. Spencer, S., Dowbenko, D., Cheng, J., Li, W., Brush, J., Utzig, S., Simanis, V., and Lasky, L. A. (1997) *J. Cell Biol.* **138,** 845–860
9. Wu, Y., Dowbenko, D., and Lasky, L. A. (1998) *J. Biol. Chem.* **273,** 30487–30496
10. Cong, F., Spencer, S., Cote, J. F., Wu, Y., Tremblay, M. L., Lasky, L. A., and Goff, S. P. (2000) *Mol. Cell* **6,** 1413–1423
11. Wang, B., Lemay, S., Tsai, S., and Veillette, A. (2001) *Mol. Cell. Biol.* **21,** 1077–1088
12. Garton, A. J., and Tonks, N. K. (1994) *EMBO J.* **13,** 3763–3771
13. Mano, H., Yamashita, Y., Sato, K., Yazaki, Y., and Hirai, H. (1995) *Blood* **85,** 343–350
14. Shiota, M., Tanihiro, T., Nakagawa, Y., Aoki, N., Ishida, N., Miyazaki, K., Ullrich, A., and Miyazaki, H. (2003) *Mol. Endocrinol.* **17,** 534–549
15. Mano, H., Yamashita, Y., Miyazato, A., Miura, Y., and Ozawa, K. (1996) *FASEB J.* **10,** 637–642
16. Mao, J., Xie, W. Yuan, H., Simon, M. I., Mano, H., and Wu, D. (1998) *EMBO J.* **17,** 5638–5646
17. Mayer, B. J., Hirai, H., and Sakai, R. (1995) *Curr. Biol.* **5,** 296–305
18. Yoshida, K., Yamashita, Y., Miyazato, A., Ohya, K., Kitanaka, A., Ikeda, U., Shimada, K., Yamanaka, T., Ozawa, K., and Mano, H. (2000) *J. Biol. Chem.* **275,** 24945–24952
19. Chen, C., and Okayama, H. (1987) *Mol. Cell. Biol.* **7,** 2745–2752
20. Yamashita, Y., Watanabe, S. Miyazato, A. Ohya, K., Ikeda, U., Shimada, K., Komatsu, N., Hatake, K., Miura, Y., Ozawa, K., and Mano, H. (1998) *Blood* **91,** 1496–1507
21. Kitanaka, A., Mano, H., Conley, M. E., and Campana, D. (1998) *Blood* **91,** 940–948
22. Machide, M., Mano, H., and Todokoro, K. (1995) *Oncogene* **11,** 619–625
23. Matsuda, T., Takahashi-Tezuka, M., Fukada, T., Okuyama, Y., Fujitani, Y., Tsukada, S., Mano, H., Hirai, H., Witte, O. N., and Hirano, T. (1995) *Blood* **85,** 627–633
24. Miyazato, A., Yamashita, Y., Hatake, K., Miura, Y., Ozawa, K., and Mano, H. (1996) *Cell Growth Differ.* **7,** 1135–1139
25. Tang, B., Mano, H., Yi, T., and Ihle, J. N. (1994) *Mol. Cell. Biol.* **14,** 8432–8437
26. Yamashita, Y., Miyazato, A., Shimizu, R., Komatsu, N., Miura, Y., Ozawa, K., and Mano, H. (1997) *Exp. Hematol.* **25,** 211–216
27. Bennett, A. M., Tang, T. L. Sugimoto, S. Walsh, C. T., and Neel, B. G. (1994) *Proc. Natl. Acad. Sci. U. S. A.* **91,** 7335–7339
28. Feng, G. S., Hui, C. C., and Pawson, T. (1993) *Science* **259,** 1607–1611
29. Vogel, W., Lammers, R. Huang, J., and Ullrich, A. (1993) *Science* **259,** 1611–1614
30. Ali, S., Chen, Z., Lebrun, J. J., Vogel, W., Kharitonenkov, A., Kelly, P. A., and Ullrich, A. (1996) *EMBO J.* **15,** 135–142
31. Boulton, T. G., Stahl, N., and Yancopoulos, G. D. (1994) *J. Biol. Chem.* **269,** 11648–11655
32. Gadina, M., Stancato, L. M., Bacon, C. M., Larner, A. C., and O'Shea, J. J. (1998) *J. Immunol.* **160,** 4657–4661
33. Tauchi, T., Feng, R., Shen, M., Hoatlin, Bagby, G. C., Jr., Kabat, D., Lu, L., and Broxmeyer, H. E. (1995) *J. Biol. Chem.* **270,** 5631–5635
34. Tauchi, T., Damen, J. E., Toyama, K., Feng, G. S., Broxmeyer, H. E., and Krystal, G. (1996) *Blood* **87,** 4495–4501
35. Welham, M. J., Dechert, U., Leslie, K. B., Jirik, F., and Schrader, J. W. (1994) *J. Biol. Chem.* **269,** 23764–23768
36. Stein-Gerlach, M., Kharitonenkov, A., Vogel, W., Ali, S., and Ullrich, A. (1995) *J. Biol. Chem.* **270,** 24635–24637
37. Stein-Gerlach, M., Wallasch, C., and Ullrich, A. (1998) *Int. J. Biochem. Cell Biol.* **30,** 559–566
38. Liu, F., and Chernoff, J. (1997) *Biochem. J.* **327,** 139–145
39. Tao, J., Malbon, C. C., and Wang, H. Y. (2001) *J. Biol. Chem.* **276,** 29520–29525
40. Mano, H., Ishikawa, F., Nishida, J., Hirai, H., and Takaku, F.(1990) *Oncogene* **5,** 1781–1786
41. Mano, H., Mano, K., Tang, B. Koehler, M., Yi, T., Gilbert, D. J., Jenkins, N. A., Copeland, N. G., and Ihle, J. N. (1993) *Oncogene* **8,** 417–424
42. Tsukada, S., Saffran, D. C., Rawlings, D. J., Parolini, O., Allen, R. C., Klisak, I., Sparkes, R. S., Kubagawa, H., Mohandas, T., Quan, S., Belmont, J. W., Cooper, M. D., Conley, M. E., and Witte, O. N. (1993) *Cell* **72,** 279–290
43. Vetrie, D., Vorechovsky, I., Sideras, P., Holland, J., Davies, A., Flinter, F., Hammarstrom, L., Kinnon, C., Levinsky, R., Bobtoe, M., Smith, C. I. E., and Bently, D. R. (1993) *Nature* **361,** 226–233
44. Heyeck, S. D., and Berg, L. J. (1993) *Proc. Natl. Acad. Sci. U. S. A.* **90,** 669–673
45. Siliciano, J. D., Morrow, T. A., and Desiderio, S. V. (1992) *Proc. Natl. Acad. Sci. U. S. A.* **89,** 11194–11198
46. Yamada, N., Kawakami, Y., Kimura, H., Fukamachi, H., Baier, G., Altman, A., Kato, T., Inagaki, Y., and Kawakami, T. (1993) *Biochem. Biophys. Res. Commun.* **192,** 231–240
47. Tamagnone, L., Lahtinen, I. Mustonen, T. Virtaneva, K., Francis, F. Muscatelli, F. Alitalo, R., Smith, C. I., Larsson, C., and Alitalo, K. (1994) *Oncogene* **9,** 3683–3688
48. Haire, R. N., and Litman, G. W. (1995) *Mamm. Genome* **6,** 476–480
49. Hu, Q., Davidson, D., Schwartzberg, P. L., Macchiarini, F., Lenardo, M. J., Bluestone, J. A., and Matis, L. A. (1995) *J. Biol. Chem.* **270,** 1928–1934
50. Ohya, K., Kajigaya, S., Kitanaka, A., Yoshida, K., Miyazato, A., Yamashita, Y., Yamanaka, T., Ikeda, U., Shimada, K., Ozawa, K., and Mano, H. (1999) *Proc. Natl. Acad. Sci. U. S. A.* **96,** 11976–11981
51. Jui, H. Y., Tseng, R. J., Wen, X., Fang, H. I., Huang, L. M., Chen, K. Y., Kung, H. J., Ann, D. K., and Shih, H. M. (2000) *J. Biol. Chem.* **275,** 41124–41132

Progress in Hematology

International Journal of
HEMATOLOGY

Stratification of Acute Myeloid Leukemia Based on Gene Expression Profiles

Hiroyuki Mano

Division of Functional Genomics, Jichi Medical School, Tochigi, Japan

Received July 28, 2004; accepted August 10, 2004

Abstract

Acute myeloid leukemia (AML) is characterized by clonal growth of immature leukemic blasts and develops either de novo or secondarily to anticancer treatment or to other hematologic disorders. Given that the current classification of AML, which is based on blast karyotype and morphology, is not sufficiently robust to predict the prognosis of each affected individual, new stratification schemes that are of better prognostic value are needed. Global profiling of gene expression in AML blasts has the potential both to identify a small number of genes whose expression is associated with clinical outcome and to provide insight into the molecular pathogenesis of this condition. Emerging genomics tools, especially DNA microarray analysis, have been applied in attempts to isolate new molecular markers for the differential diagnosis of AML and to identify genes that contribute to leukemogenesis. Progress in bioinformatics has also yielded means with which to classify patients according to clinical parameters such as long-term prognosis. The application of such analysis to large sets of gene expression data has begun to provide the basis for a new AML classification that is more powerful with regard to prediction of prognosis.
Int J Hematol. 2004;80:389-394. doi: 10.1532/IJH97.04111

Key words: DNA microarray; CD133; CD34; Transcriptome

1. Introduction

The human genome project was launched in 1991 as a joint program by the United States, the United Kingdom, Japan, France, Germany, and China. Ten years later, the first draft sequence of the entire human genome, including the nucleotide sequence of approximately 90% of euchromatin with 99.9% accuracy, was completed by the international team [1]. The total number of protein-coding genes was estimated to be approximately 31,000, only twice that for a nematode [2]. Completion of the human sequencing project was announced in 2003, with the determined nucleotide sequence encompassing >99% of euchromatin with an accuracy of 99.99% (http://www.ncbi.nlm.nih.gov/genome/guide/human). Annotation of the final sequence is still in progress but is expected to be completed soon. The postgenome era is therefore about to begin.

Compilation of the catalog of human genes has spurred the development of new technologies to investigate and characterize changes—at the gene, messenger RNA (mRNA), or protein level—in the entire gene set simultaneously. Among such genomics approaches, DNA microarray analysis has probably been the most successful to date. A DNA microarray resembles a microscope slide and contains tens of thousands of genomic fragments, complementary DNAs (cDNAs), or oligonucleotides present in individual spots. Hybridization of such arrays with labeled cDNAs derived from a sample mRNA population allows measurement of the amounts of the original mRNAs for all genes represented on the array [3]. The high density of DNA fragments achievable on currently available microarrays makes it possible to quantitate the mRNA levels for all human genes with 1 array experiment. Such profiling of gene expression in a given cell or tissue type promises to provide a new dimension to our understanding of biology.

Microarray analysis has been applied, for instance, to characterize the differentiation [4] and the inflammatory response [5] of human cells. Gene expression profiling has also helped to develop new classification systems for human diseases that had previously been categorized on the basis of pathology or cell morphology. Microarray analysis of human specimens of prostate cancer, for example, has resulted in the identification of new biomarkers that predict poor prognosis [6]. Characteristic patterns of gene expression, or "molecular signatures," are similarly expected to provide a basis for the subdivision of patients with the same clinical diagnosis into groups with distinct prognoses [7].

Acute myeloid leukemia (AML) is characterized by the clonal growth of immature leukemic blasts in bone marrow

Correspondence and reprint requests: Hiroyuki Mano, MD, PhD, Division of Functional Genomics, Jichi Medical School, 3311-1 Yakushiji, Kawachigun, Tochigi 329-0498, Japan; 81-285-58-7449; fax: 81-285-44-7322 (e-mail: hmano@jichi.ac.jp).

(BM) and can develop de novo or from either myelodysplastic syndrome (MDS) or anticancer treatment [8]. One of the most robust predictors of AML prognosis is blast karyotype [9,10]. A good prognosis is thus predicted from the presence in leukemic clones of t(8;21), t(15;17), or inv(16) chromosomal rearrangements, whereas –7/7q–, 11q23, or more complex abnormalities are indicative of a poor outcome. Such stratification is not informative, however, for predicting the prognoses of patients with a normal karyotype, who constitute approximately 50% of the AML population.

A clinical record of a preceding MDS phase is also an indicator of poor prognosis for individuals with AML. Therapy-related acute leukemia (TRL) can develop after the administration of alkylating agents, topoisomerase inhibitors, or radiotherapy. The clinical outcome of TRL is generally worse than that of de novo AML [11], and a subset of individuals with TRL also exhibits multilineage dysplasia of blood cells. Prediction of the outcome of and optimization of the treatment for each AML patient would thus be facilitated by the ability to differentiate de novo AML from MDS-related AML and TRL. However, dysplastic changes (in particular, dyserythropoiesis) in differentiated blood cells are also found not infrequently in the BM of healthy elderly individuals [12]. The differential diagnosis among AML-related disorders is therefore not always an easy task in the clinical setting, especially if a prior record of hematopoietic parameters is not available.

The application of DNA microarray analysis to AML has the potential (1) to identify molecular markers for the differential diagnosis of AML-related disorders, (2) to provide a basis for the subclassification of such disorders, and (3) to yield insight into the molecular pathogenesis of AML. In this article, I review progress related to the first 2 of these goals.

2. Identification of Molecular Markers for the Differential Diagnosis of AML

2.1. Karyotype

Given that the current classification of AML relies on blast karyotype, it would be informative to determine whether karyotype is related to the gene expression profile of blasts. In other words, is DNA microarray analysis able to substitute for conventional karyotyping?

Schoch et al performed microarray analysis with BM mononuclear cells (MNCs) isolated from individuals with AML and compared the data among the patients with t(8;21), t(15:17), or inv(16) chromosomal anomalies [13]. Each of these 3 AML subgroups was found to possess a distinct molecular signature, and it was possible to predict the karyotype correctly on the basis of the expression level of specific genes. The leukemic blasts of these subgroups of AML manifest distinct differentiation abilities, however. Blasts with t(8;21) remain as immature myeloblasts, those with t(15;17) differentiate into promyelocytes, and those with inv(16) differentiate into cells of the monocytic lineage. The overall gene expression profiles of these 3 types of blasts therefore might be substantially affected by the mRNA repertoires of the differentiated cells present within BM. It remains to be determined whether such "karyotype-specific" molecular signatures are indeed dependent on karyotype or are related to French-American-British (FAB) subtype (differentiation ability).

The gene expression profiles of BM MNCs derived from a large number of pediatric AML patients were examined by Yagi et al [14]. Clustering of these patients according to the expression pattern of the entire gene set resulted in their separation into FAB subtype–matched groups, indicative of a prominent influence of differentiated cells within BM on the gene expression profile. It may nevertheless prove possible to capture bona fide karyotype-dependent genes from large data sets with the use of sophisticated bioinformatics approaches and then to use the expression profiles of these genes for "pseudokaryotyping."

Virtaneva et al purified $CD34^+$ progenitor cells from the BM of individuals with AML and compared the gene expression profiles of the patients with a normal karyotype and those with trisomy 8 [15]. They also compared such AML blasts with $CD34^+$ fractions isolated from the BM of healthy volunteers. The use of $CD34^+$ (immature) cells for microarray analysis would be expected to reduce the influence of differentiated cells within BM on the overall pattern of gene expression. These researchers found that the AML blasts differed markedly from normal $CD34^+$ cells in terms of the gene expression profile. However, the blasts with trisomy 8 did not appear to differ substantially from those with a normal karyotype. It is possible that blasts with a normal karyotype or those with trisomy 8 are too diverse to allow identification of distinguishing gene markers.

2.2. De Novo AML versus MDS-Related AML

Although dysplasia is the diagnostic hallmark of MDS, such abnormal cell morphology is also associated with other conditions, and the subjective assessment of the extent of dysplasia suffers from the risk of variability from physician to physician. It is therefore desirable to identify molecular markers that are able to distinguish de novo AML from MDS-associated AML. It is also important to clarify whether de novo AML and MDS-associated AML are indeed distinct clinical entities or whether they overlap to some degree.

Although DNA microarray analysis is a promising tool for the identification of such molecular markers able to differentiate de novo AML from MDS-related AML, a simple comparison of BM MNCs for these 2 conditions is likely to be problematic. The cellular composition of BM MNCs differs markedly among individuals. Differences in the gene expression profile between BM MNCs from a given pair of individuals may thus reflect these differences in cell composition [16]. The elimination of such pseudopositive and pseudonegative data necessitates the purification of background-matched cell fractions from the clinical specimens before microarray analysis.

Given that de novo AML and MDS both result from the transformation of hematopoietic stem cell (HSC) clones, HSCs would be expected to be an appropriate target for purification and gene expression analysis. With the use of an affinity purification procedure based on the HSC-specific surface protein CD133, also known as AC133 [17], we have purified $CD133^+$ HSC-like fractions from individuals with

various hematopoietic disorders, and we have stored these fractions in a cell depository referred to as the *Blast Bank*. With such background-matched purified samples, we attempted to identify differences in gene expression profiles between de novo AML and MDS-associated AML [18]. To minimize further the influence of differentiation commitment of blasts toward certain lineages, we used only Blast Bank samples with the same phenotype, the M2 subtype according to the FAB classification. We thus characterized the expression profiles of >12,000 genes in $CD133^+$ Blast Bank samples from 10 patients with de novo AML of the M2 subtype as well as from 10 individuals with MDS-related AML of the same FAB subtype.

Selection with a Student t test ($P < .01$) and an effect size of ≥ 5 units for discrimination between the 2 clinical conditions led to the identification of 57 "diagnosis-associated genes," the expression profiles of which are shown in a "gene tree" format in Figure 1A. In this format, genes with similar expression patterns across the samples are clustered near each other. Patients were also clustered in this tree (2-way clustering) on the basis of the similarity of the expression pattern of the 57 genes (dendrogram at the top). All subjects were clustered into 2 major groups, 1 composed mostly of de novo AML patients and the other containing predominantly patients with MDS-associated AML. Each of these 2 main branches contained misclassified samples, however, indicating that simple clustering was not sufficiently powerful to differentiate the 2 clinical conditions completely. Furthermore, this analysis might not adequately address whether de novo AML and MDS-associated AML should be treated as distinct entities, at least from the point of view of the gene expression profile.

Decomposition of the multidimensionality of gene expression profiles by the application of principal components analysis [19] or correspondence analysis [20], for example, is often informative for such purposes. Application of the latter method to the data set of the 57 genes reduced the number of dimensions from 57 to 3. On the basis of the calculated 3-dimensional (3D) coordinates for each sample, the specimens were then projected into a virtual 3D space (Figure 1B). Most of the de novo AML samples were positioned in a region of this space that was distinct from that occupied by the MDS-associated AML specimens. However, 2 of the former samples were localized within the MDS region. These results suggest that de novo AML and MDS-associated AML are distinct disorders but that the current clinical diagnostic system is not efficient enough to separate them completely.

Instead of extracting a molecular signature from the expression profile of multiple genes, an alternative approach is to attempt to identify individual gene markers specific to either de novo AML or MDS-associated AML. We used the Blast Bank array data to identify MDS-specific markers, defined as genes that are silent in blasts from all de novo AML patients but are active in those from at least some patients with MDS-related AML [16]. This approach resulted in the identification of a single gene, *DLK*, that matched these criteria. *DLK* is expressed in immature cells [21] and is implicated in the maintenance of the undifferentiated state [22]. Selective expression of *DLK* in MDS blasts may thus contribute to the pathogenesis of MDS. Increased expression

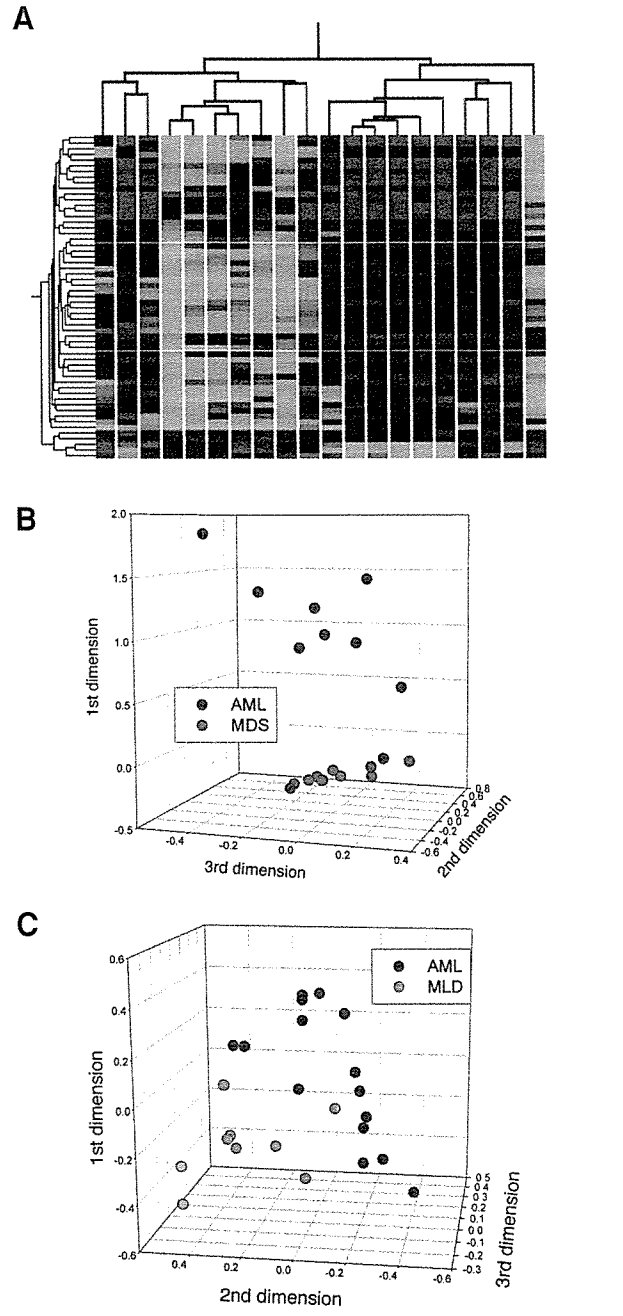

Figure 1. Correspondence analysis and 3-dimensional (3D) projection for differential diagnosis of acute myeloid leukemia (AML). A, Two-way hierarchical clustering for 57 disease-associated genes and 20 patients. Each row corresponds to a single gene and each column to $CD133^+$ cells from a patient with de novo AML (blue) or myelodysplastic syndrome (MDS)-related AML (red). The expression level of each gene is color coded, with a high level in red and a low level in green. B, Projection of the 20 specimens from (A) into a virtual space with 3 dimensions identified by correspondence analysis of the 57 genes. Patients with de novo AML (AML) were separated from those with MDS-related leukemia (MDS). C, Projection of specimens from patients with de novo AML without dysplasia (AML) or de novo AML with multilineage dysplasia (MLD) into a 3-dimensional space based on correspondence analysis of differences in gene expression. The dendrogram in (A) and 3-dimensional projections in (B) and (C) were constructed from data in [18] and [28].

of *DLK* in blasts from individuals with MDS has also been demonstrated in other studies [18,23].

Cell fractions other than $CD133^+$ cells are also potential targets for microarray analysis. Pellagatti et al chose peripheral blood neutrophils to investigate the gene expression profiles of MDS and MDS-associated AML [24]. They identified genes whose expression was dependent on MDS subtype. Given the high activity of ribonuclease in neutrophils, however, it is important to confirm the reproducibility of expression data obtained with these cells.

2.3. Dysplasia

In addition to the dysplastic blood cells associated with MDS, prominent dysplasia is apparent in certain individuals with de novo AML for whom the possibility of a prior MDS phase can be excluded [25,26]. Such de novo AML with dysplasia has a poor outcome with conventional chemotherapy [27], as does MDS-related leukemia. In the revised classification of AML by the World Health Organization [8], an entity of AML with multilineage dysplasia (AML-MLD) has been proposed; this entity probably includes both de novo AML with dysplasia and AML secondary to MDS. Whether such an amalgamation has clinical relevance awaits further studies.

To clarify directly whether de novo AML-MLD is indeed a clinical entity distinct from de novo AML without dysplasia, we searched for differences between the transcriptomes of $CD133^+$ cells derived from individuals with diagnoses of these 2 conditions [28]. We attempted to construct a 3D view of the samples with the coordinates calculated from correspondence analysis of genes found to be associated with dysplasia (Figure 1C). Most cases of AML-MLD were separated from those of AML without dysplasia in the 3D space. In contrast to the prominent separation power of the first dimension in Figure 1B, both the first and second dimensions substantially contributed to separation of the samples in Figure 1C. These data indicate that de novo AML without dysplasia can be differentiated from de novo AML-MLD on the basis of gene expression profiles.

3. Stratification of AML

3.1. Analysis of BM MNCs

Given that the current classification of AML is not sufficiently powerful to predict the prognosis of each affected individual, it is hoped that DNA microarray analysis will provide a better stratification scheme to separate AML patients into prognosis-dependent subgroups. To this end, Bullinger et al isolated MNCs from either BM or peripheral blood of 116 adult AML patients and examined the gene expression profiles of these cells with DNA microarrays harboring >39,000 cDNAs [29]. From the data set, they then screened "class predictor" genes, whose expression was correlated with the duration of patient survival. Class prediction based on such genes separated the patients into 2 classes, and long-term survival differed significantly between these 2 classes for both the training set ($P < .001$, log-rank test) and the test set ($P = .006$). This expression profile–based classification also separated AML patients with normal karyotype into 2 classes with distinct prognoses ($P = .046$). Although the number of genes used for the class prediction was relatively large (n = 133), these data demonstrated that DNA microarray analysis is able to predict the prognosis of AML patients in a manner independent of karyotype.

Similarly, Valk et al measured the expression levels of approximately 13,000 genes in BM MNCs isolated from 285 patients with AML [30]. Unsupervised clustering based on the gene expression profiles separated the patients into 16 subgroups. The prognoses of patients differed among these clusters, but whether the ability to predict prognosis was independent of karyotype was not addressed.

The gene expression profiles of BM MNCs from 54 pediatric AML patients were compared for those individuals who maintained complete remission (CR) for >3 years and those who failed to enter initial CR [14]. Thirty-five genes were identified as associated with prognosis and were used to separate the individuals into 2 groups. The difference in survival between the 2 groups was again statistically significant ($P = .03$), although whether this approach was independent of the current classification system was not addressed.

3.2. Analysis of Purified Fractions

As described in section 2.2, microarray analysis of purified fractions is likely to be more accurate than is that of BM MNCs for the extraction of prognosis-associated molecular signatures. We have analyzed the expression intensities of approximately 33,000 genes (likely representing almost the entire human genome) in $CD133^+$ HSC-like fractions isolated from 66 patients with AML who received standard chemotherapy. Of these patients, 51 individuals entered initial CR, whereas the remaining 15 failed to do so. Comparison of the data set for these 2 classes resulted in the identification of a small number of outcome-related genes (Yamashita et al, unpublished data). Principal components were extracted from the gene expression patterns, and the patients were projected into a virtual 3D space based on the coordinates obtained by correspondence analysis. Individuals who entered CR were separated from those who did not (Figure 2A), indicating that the gene expression profile of leukemic blasts indeed differs between AML patients who respond to chemotherapy and those who do not. In this analysis, the separation of the 2 groups of patients was achieved mostly in the first dimension. We therefore separated the patients into 2 subgroups according to whether the coordinate in the first dimension was <-0.3 or ≥ -0.3. The individuals in the latter group lived significantly longer than did those in the former (Figure 2B). These data support the feasibility of a novel stratification scheme for AML based on the gene expression profile.

4. Conclusion

Newly developed genomics tools allow global assessment of mRNA levels, DNA copy number, or genomic polymorphisms. Among these tools, DNA microarray analysis has proved highly successful in studies of human specimens, not only from individuals with hematopoietic disorders but also

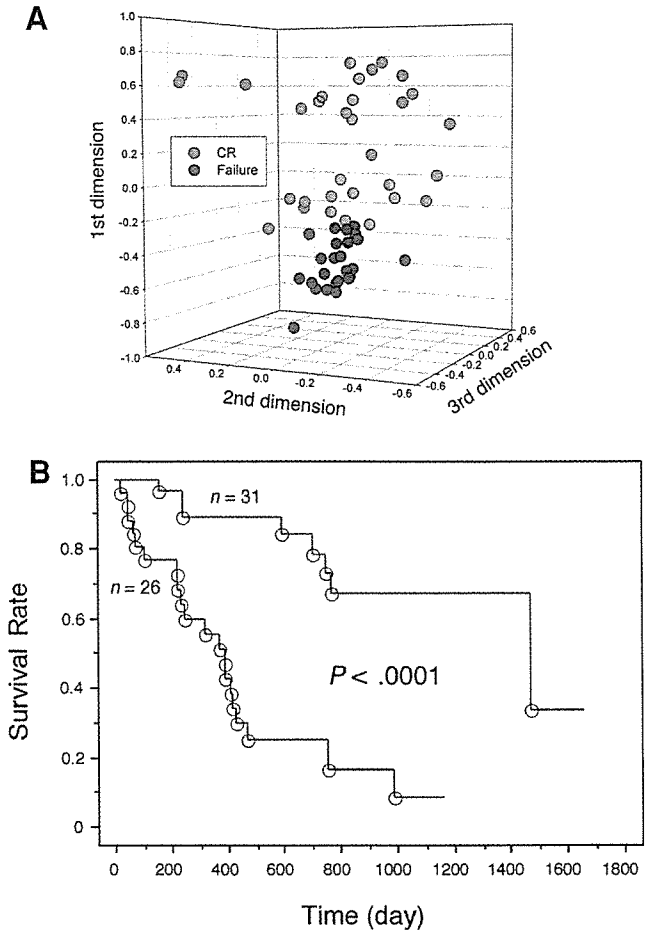

Figure 2. Stratification of acute myeloid leukemia (AML) on the basis of microarray analysis of gene expression. A, Projection of specimens from patients with AML who underwent initial chemotherapy-induced complete remission (CR) and those who did not (Failure) into a 3-dimensional space based on correspondence analysis of differences in gene expression. B, Kaplan-Meier analysis of the subjects in (A), revealing significantly different prognoses for the 2 classes with a coordinate in the first dimension of <–0.3 or ≥–0.3.

from those with solid tumors or nonmalignant degenerative diseases. Insight into many more human disorders is likely soon to be provided by such global profiling of gene expression. It is important to bear in mind, however, that DNA microarray data are prone to contamination with pseudopositive or pseudonegative results. The efficient characterization of AML thus appears to require optimal purification of target cell populations. Provided that experiments are designed carefully, DNA microarray analysis is likely to shed new light on the molecular pathogenesis of AML.

Acknowledgments

I thank colleagues in the Division of Functional Genomics, Jichi Medical School, for their enthusiasm in DNA microarray analyses, as well as the many physicians and patients who have participated in the Blast Bank project.

References

1. The Genome International Sequencing Consortium. Initial sequencing and analysis of the human genome. *Nature*. 2001;409: 860-921.
2. The *C. elegans* Sequencing Consortium. Genome sequence of the nematode *C. elegans*: a platform for investigating biology. *Science*. 1998;282:2012-2018.
3. Cheung VG, Morley M, Aguilar F, Massimi A, Kucherlapati R, Childs G. Making and reading microarrays. *Nat Genet*. 1999;21: 15-19.
4. Khan J, Bittner ML, Saal LH, et al. cDNA microarrays detect activation of a myogenic transcription program by the *PAX3-FKHR* fusion gene. *Proc Natl Acad Sci U S A*. 1999;96:13264-13269.
5. Heller RA, Schena M, Chai A, et al. Discovery and analysis of inflammatory disease-related genes using cDNA microarrays. *Proc Natl Acad Sci U S A*. 1997;94:2150-2155.
6. Dhanasekaran SM, Barrette TR, Ghosh D, et al. Delineation of prognostic biomarkers in prostate cancer. *Nature*. 2001;412: 822-826.
7. Beer DG, Kardia SL, Huang CC, et al. Gene-expression profiles predict survival of patients with lung adenocarcinoma. *Nat Med*. 2002;8:816-824.
8. Jaffe ES, Harris NL, Vardman JW, eds. *Tumours of Haematopoietic and Lymphoid Tissues*. Lyon, France: IARC Press; 2001.
9. Grimwade D, Walker H, Oliver F, et al. The importance of diagnostic cytogenetics on outcome in AML: analysis of 1,612 patients entered into the MRC AML 10 trial: the Medical Research Council Adult and Children's Leukaemia Working Parties. *Blood*. 1998; 92:2322-2333.
10. Byrd JC, Mrozek K, Dodge RK, et al. Pretreatment cytogenetic abnormalities are predictive of induction success, cumulative incidence of relapse, and overall survival in adult patients with de novo acute myeloid leukemia: results from Cancer and Leukemia Group B (CALGB 8461). *Blood*. 2002;100:4325-4336.
11. Smith SM, Le Beau MM, Huo D, et al. Clinical-cytogenetic associations in 306 patients with therapy-related myelodysplasia and myeloid leukemia: the University of Chicago series. *Blood*. 2003; 102:43-52.
12. Bain BJ. The bone marrow aspirate of healthy subjects. *Br J Haematol*. 1996;94:206-209.
13. Schoch C, Kohlmann A, Schnittger S, et al. Acute myeloid leukemias with reciprocal rearrangements can be distinguished by specific gene expression profiles. *Proc Natl Acad Sci U S A*. 2002;99: 10008-10013.
14. Yagi T, Morimoto A, Eguchi M, et al. Identification of a gene expression signature associated with pediatric AML prognosis. *Blood*. 2003;102:1849-1856.
15. Virtaneva K, Wright FA, Tanner SM, et al. Expression profiling reveals fundamental biological differences in acute myeloid leukemia with isolated trisomy 8 and normal cytogenetics. *Proc Natl Acad Sci U S A*. 2001;98:1124-1129.
16. Miyazato A, Ueno S, Ohmine K, et al. Identification of myelodysplastic syndrome-specific genes by DNA microarray analysis with purified hematopoietic stem cell fraction. *Blood*. 2001;98:422-427.
17. Hin AH, Miraglia S, Zanjani ED, et al. AC133, a novel marker for human hematopoietic stem and progenitor cells. *Blood*. 1997;90: 5002-5012.
18. Oshima Y, Ueda M, Yamashita Y, et al. DNA microarray analysis of hematopoietic stem cell-like fractions from individuals with the M2 subtype of acute myeloid leukemia. *Leukemia*. 2003;17: 1990-1997.
19. Lefkovits I, Kuhn L, Valiron O, Merle A, Kettman J. Toward an objective classification of cells in the immune system. *Proc Natl Acad Sci U S A*. 1988;85:3565-3569.
20. Fellenberg K, Hauser NC, Brors B, Neutzner A, Hoheisel JD, Vingron M. Correspondence analysis applied to microarray data. *Proc Natl Acad Sci U S A*. 2001;98:10781-10786.
21. Moore KA, Pytowski B, Witte L, Hicklin D, Lemischka IR.

Hematopoietic activity of a stromal cell transmembrane protein containing epidermal growth factor-like repeat motifs. *Proc Natl Acad Sci U S A*. 1997;94:4011-4016.
22. Smas CM, Sul HS. Pref-1, a protein containing EGF-like repeats, inhibits adipocyte differentiation. *Cell*. 1993;73:725-734.
23. Hofmann WK, de Vos S, Komor M, Hoelzer D, Wachsman W, Koeffler HP. Characterization of gene expression of $CD34^+$ cells from normal and myelodysplastic bone marrow. *Blood*. 2002;100: 3553-3560.
24. Pellagatti A, Esoof N, Watkins F, et al. Gene expression profiling in the myelodysplastic syndromes using cDNA microarray technology. *Br J Haematol*. 2004;125:576-583.
25. Brito-Babapulle F, Catovsky D, Galton DAG. Clinical and laboratory features of de novo acute myeloid leukemia with trilineage myelodysplasia. *Br J Haematol*. 1987;66:445-450.
26. Jinnai I, Tomonaga M, Kuriyama K, et al. Dysmegakaryocytopoiesis in acute leukaemias: its predominance in myelomonocytic (M4) leukaemia and implication for poor response to chemotherapy. *Br J Haematol*. 1987;66:467-472.
27. Kuriyama K, Tomonaga M, Matsuo T, et al. Poor response to intensive chemotherapy in de novo acute myeloid leukaemia with trilineage myelodysplasia: Japan Adult Leukaemia Study Group (JALSG). *Br J Haematol*. 1994;86:767-773.
28. Tsutsumi C, Ueda M, Miyazaki Y, et al. DNA microarray analysis of dysplastic morphology associated with acute myeloid leukemia. *Exp Hematol*. 2004;32:828-835.
29. Bullinger L, Dohner K, Bair E, et al. Use of gene-expression profiling to identify prognostic subclasses in adult acute myeloid leukemia. *N Engl J Med*. 2004;350:1605-1616.
30. Valk PJ, Verhaak RG, Beijen MA, et al. Prognostically useful gene-expression profiles in acute myeloid leukemia. *N Engl J Med*. 2004; 350:1617-1628.

Annual Review 血液 2004

2004 年 1 月 30 日 発行

中外医学社

5. 多発性骨髄腫と関連疾患の遺伝子発現プロファイル

自治医科大学ゲノム機能研究部教授　間野博行

key words　DNA microarray, multiple myeloma, MGUS, CD138

動　向

多発性骨髄腫（multiple myeloma: MM）は形質細胞の異常増殖を本体とする悪性疾患であり高齢者に好発する[1]．MMはきわめて予後不良であり，ほとんどの例において最終的には化学療法に抵抗性となる[2]．一方，以前は良性単クローン性免疫グロブリン血症とよばれていたmonoclonal gammopathy of undetermined significance（MGUS）は，MMに比べて骨髄中の形質細胞の割合が少なく，また一般に全身症状も伴わない．しかしMGUS患者の中には1年に1%程度の割合でMMへ移行する症例が存在しており，MGUSとMMとの異同はいまだ不明確である[3]．MGUSは前癌状態ともいうべきものなのか，それともMGUSは不均一な集団であり一部の特徴的なサブグループのみがMMへ移行するのか，またMGUSとMMとを区別するgenetic eventsは果たして何なのか？など疑問点は多い．

一方，MMも発症当初は化学療法が比較的奏効し，一旦は症状が軽減するが，化学療法自体でMM細胞が根治されることはほとんどなく，早晩，患者骨髄腫細胞は化学療法に抵抗性となる．現段階でMMの生命予後を明確に改善する治療法は骨髄移植のみであり[4]，それも自家と同種のどちらが優れているかは議論の多いところである[5]．

比較的罹患人口の多い疾患にもかかわらず，MMの病態はほとんど不明なままである．このようなMMの発症機構を明らかにし，同時に各患者の予後を予測することを目的として，DNAチップを用いた新しいアプローチが複数の施設から報告されるようになった．これらの解析結果はいまだ必ずしも画期的とはいえないが，MMに関して全く新しい側面からの知見が急速に蓄積されつつあることは間違いない．本稿ではMM細胞の起源あるいはMM患者のサブグループの提言など，これらのチップ解析の結果得られた情報について概説したい．

A. 遺伝子発現プロファイル

ヒトゲノムプロジェクトの成果であるドラフトシークエンスが2001年2月に公表され[6,7]，またついにeuchromatinの完全版配列決定が2003年4月14日に宣言された．現在，得られた配列上に遺伝子の割付作業が行われているが，近い将来にその成果が公表されると思われる．ヒトのほとんどの遺伝子構造が（機能は不明であるにしろ）明らかになった今後の「ポスト・ゲノム時代」においては医療・医学研究の分野でも方法論の転換が

求められるであろう．たとえばある疾患の原因遺伝子を同定することを考えるとき，旧来であれば発現スクリーニング法や連鎖解析法などによって全く未知の遺伝子を最初から同定せざるを得なかった．しかしポスト・ゲノム時代においては理論上「未知」の遺伝子は存在しなくなり，膨大ではあるがあくまで有限なヒト遺伝子のプールの中から特定の特徴を備えた遺伝子を効率よく同定することが必要になる．このような網羅的解析は，DNAシークエンス，遺伝子発現量（mRNA量）および蛋白質の全ての段階で行われるであろう．この中で現在すでに強力な網羅的解析技術が存在するのは「遺伝子発現量」の分野であり，その技術とはDNAチップである．

DNAチップはスライドガラスなどの担体の上に，cDNAあるいは遺伝子由来のオリゴヌクレオチドを高密度に配置したものであり，スライド上の数千から数万種類の遺伝子の相対的発現量を一度の実験で解析することができる[8]．すでにデータベース上に存在するヒトの全予想遺伝子を配置したDNAチップも市販されており（http://www.affymetrix.com），これらの高密度DNAチップを用いることで，たとえば任意の細胞・組織における全遺伝子の発現パターン（遺伝子発現プロファイル）も比較的簡便に把握可能となる．geneに「全体」を表す「-ome」という接尾語を付けてgenome（ゲノム）という単語が作られたように，transcriptに-omeを付加したtranscriptome（トランスクリプトーム）という造語も最近は用いられるようになった．

このような遺伝子発現プロファイル・トランスクリプトームをたとえばMMとMGUS間で大規模に比較することで，両者を鑑別可能な新しい分子診断マーカーの同定も可能になると期待される．またDNAチップによって得られる発現データを用いて，疾患の分類自体に新しい体系を導入することも可能であろう．

B. CD138陽性分画を用いた比較

しかし，たとえば健常者とMM患者骨髄単核球（mononuclear cell: MNC）を単純に比較するようなDNAチップ実験を行うと，意外にも本アッセイが偽陽性の多い解析法であることに気づく．形質細胞は健常者骨髄中で数%を占めるに過ぎないが，MM患者においては時に数十%に及ぶ．したがって骨髄MNC間で比較すると，形質細胞固有な遺伝子はMM患者において見かけ上必ず発現が誘導されているように結論づけられてしまうのである．このような偽陽性結果を回避するためには，疾患責任分画である形質細胞のみを様々な患者より純化した上で，DNAチップによって比較することが重要であろう．Bリンパ球は成熟形質細胞への分化に伴い細胞表面CD19，CD20の発現量が低下し，逆にCD138，CD38の発現が誘導される．特にCD138は骨髄中の血球において成熟形質細胞にのみ発現しており，同細胞分画を純化するのに好適である[9]．

そこで我々を含め複数の研究グループにおいて，健常者，MGUS患者及びMM患者骨髄よりCD138陽性形質細胞を純化しDNAチップによって比較するプロジェクトが進行した．具体的なCD138陽性細胞の純化ステップとして，抗CD138抗体に磁気ビーズを結合させた純化カラムが用いられている．フローサイトメーターを用いた細胞分画の純化も可能であるが，たとえば1×10^6個のCD138陽性細胞をFACSによって純化するのは長時間を要する．それに比べて磁気ビーズカラムを用いれば同程度の細胞の純化も1時間以内に回収可能である．磁気ビーズカラムによる細胞純化の効率を図1に示す．たとえば本解析における健常者の骨髄MNC中CD138陽性細胞は1.8%しか存在しないが，同じ健常者MNCを純化カラムにかけると最終的にCD138陽性細胞94.9%のきわめて純度の高い形質細胞分画が得られるの

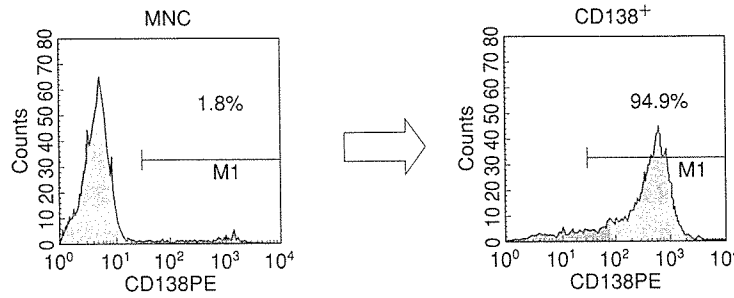

図1　CD138陽性細胞の純化

健常者より単核球（MNC）を純化し，さらに抗CD138抗体を用いた磁気ビーズカラムによりCD138陽性細胞（CD138$^+$）を純化した．両分画に対してFITC結合抗CD138抗体によるFACS解析を行ったヒストグラムを表す．それぞれにおけるCD138陽性細胞の割合も%で示してある．

である．同分画のサイトスピン標本をWright-Giemsa染色にて鏡検すると，均質な形質細胞のみが純化されていることが確認された．

C. 多発性骨髄腫の解析

1. 免疫グロブリンサブタイプでの比較

Magrangeasらは，88例のMM患者および9例の形質細胞性白血病（plasma cell leukmia: PCL）患者骨髄よりCD138陽性形質細胞を純化し，各サンプルより放射標識したcDNAを作成してカスタムメイドのcDNAマクロアレイ（5376遺伝子）にハイブリダイズさせた[10]．得られた遺伝子発現プロファイルをMMの異常免疫グロブリンのサブタイプ間で比較している．たとえば産生グロブリンがIgGであるもの（48例）とIgA（21例）とで比較し，両者を識別する発現プロファイルをもつ遺伝子群を抽出した．これらには免疫グロブリン関連遺伝子だけでなく，GATA6やLKF1等の転写因子，またBRCA1等のがん抑制遺伝子も含まれていた．またこれらサブタイプ依存性遺伝子セットにおける遺伝子発現パターンの類似性から，サンプルの系統樹を作成するとBence Jones proteinタイプのMM患者はIgG，IgA産生型いずれとも異なる別の疾患グループを形成することがわかった．

また彼らは産生される免疫グロブリンのL鎖のサブタイプによる比較も行っている．λ鎖産生MMとκ鎖産生型との間で発現量に偏りがある遺伝子を抽出したところ，κ鎖産生MM細胞においてMIP1α[11]，TGFβ3，BMP2などの骨代謝に関係する遺伝子群が特異的に発現していることが示された．一方，λ鎖型ではTGFβ機能を抑制するLTBP4遺伝子が特異的に発現することが示された（表1）．これらはMM細胞で産生されるL鎖のタイプ依存性に骨病変の重症度が異なる可能性を示唆する．そこでこれらL鎖依存性遺伝子の発現プロファイルを元に患者サンプルを並び替え，系統樹を作成すると，図2に示されるように骨病変が軽症の患者サンプルの多くはλ鎖産生グループに分類され，一方，骨病変が重症な患者サンプルの多くはκ鎖グループに分類されることが明らかになった．これまでもL鎖のサブタイプがMM患者における骨融解の程度にリンクするとの臨床情報があったが[12]，Magrangeasらのデータは，分子生物学的な裏づけを与えるものとして興味深い．

表1　λ鎖型とκ鎖型で発現が異なる遺伝子[10]

gene symbol	gene description	accession no.	discriminating score
IGL@	Ig λ	H14524	− 2.74
IGL@	Ig λ	R83196	− 1.81
CDSN	corneodesmosin	W95594	− 1.77
MCP	membrane cofactor protein (CD46)	H26673	− 1.66
IGL@	Ig λ	H15030	− 1.62
ABCD4	ATP-binding cassette, subfamily D, member 4	H51632	− 1.22
SAMHD1	SAM domain and HD domain, 1	H47862	− 1.07
LTBP4	latent transforming growth factor-β-binding protein 4	R73631	− 1.02
TGF3	transforming growth factor, β-3	W80655	0.73
TNFRSF6	tumor necrosis factor receptor superfamily, member 6 (CD95)	AA031300	1.06
BMP2	bone morphogenetic protein 2	AA114112	1.34
PRKCABP	PRKCA-binding protein	AA641722	1.54
HOX11	homeobox 11	AA007444	1.61
EXT1	exostoses, multiple, type 1	R13402	1.70
IGKC	Ig κ	R71916	1.82

discriminating scoreは両群における平均値の差を標準偏差の差で割ったもので，両群間における発現量の偏りを表す．

2．疾患サブタイプでの比較

Zhanらは，健常者31例，MGUS患者5例およびMM患者74例の骨髄よりCD138陽性形質細胞分画を純化し，Affymetrix社のGeneChip HuGeneFLチップ（～6800遺伝子）による解析を行った．また同様に8種類の多発性骨髄腫細胞株についてもチップ解析を行っている．これら計118例のチップデータを基にサンプル全体の系統樹を作成すると，健常者は「MGUS＋MM＋細胞株」群とは異なるグループを形成することが示され，遺伝子発現プロファイルによる疾患解析の妥当性が支持される結果となった[13]．

さらにMM内でのみサンプルの系統樹を作成すると，図3に示されるように大きく4種類の患者サブグループ（MM1～MM4）に分かれることが明らかになった．しかもMM1はMGUSに最も近い遺伝子発現プロファイルをもち，MM4は骨髄腫細胞株に最も近似したプロファイルをもつことも示された．すなわちMM内のこれらサブタイプが患者の予後にリンクする可能性が示唆される．実際MM1とMM4タイプ間で最も発現量が異なる遺伝子をリストすると，DNA複製や修復に関わる遺伝子群［thymidylate synthase（TYMS），mutS homolog 2（MSH2）等］がMM4グループに特異的に発現していることがわかる（表2）．これらのデータはMM4に属する骨髄腫細胞の増殖能力が亢進していることを支持するといえよう．またMM患者における既知の予後不良因子である血中β_2ミクログロブリン[14]，クレアチニンレベルの増加は，ともにMM4群において顕著なことも確認された．

Zhanらは，同じデータセットから正常形質細胞とMM細胞との比較も行っている．たとえば骨髄腫の細胞において特異的に発現する遺伝子として，cyclin-dependent kinase inhibitor 1A，c-Ablキナーゼ等が疾患特異的に発現亢進していることが確認された．以上の実験結果から，遺伝子発現プロファイルによって正常形質細胞と異常（MGUS＋MM）を区別することは可能であったが，MGUSとMMとを正確に判別することは困難であると結論づけられた．